Renewable and Sustainable Energy Reviews 15 (2011) 1403–1426

Contents lists available at ScienceDirect

Renewable and Sustainable Energy Reviews

journal homepage: www.elsevier.com/locate/rser

Measurement of total and spectral solar irradiance: Overview of existing research

Yousef A. Eltbaakh [a,*], M.H. Ruslan [b], M.A. Alghoul [b], M.Y. Othman [b], K. Sopian [b], M.I. Fadhel [b]

[a] Physics Department, Universiti Kebangsaan Malaysia, 43600 Bangi, Selangor, Malaysia
[b] Solar Energy Research Institute, Universiti Kebangsaan Malaysia, 43600 Bangi, Selangor, Malaysia

ARTICLE INFO

Article history:
Received 19 May 2010
Accepted 26 October 2010
Available online 12 January 2011

Keywords:
Solar
Terrestrial
Extraterrestrial
Spectrum
Broadband
Visible
UV
Near IR

ABSTRACT

The quantitative assessments of the solar radiation flux and the variations of its spectral distribution in the visible and near-infrared ranges of the electromagnetic spectrum are of great interest in studying solar–terrestrial influences. The reason is that the main part of the solar radiation energy is concentrated in that range and it determines the thermal equilibrium of the earth's atmosphere. This paper provides an overview of spectral global solar irradiance observations and of broadband solar irradiance observations from the ultraviolet to the near infrared. Measurements of the spectral solar irradiance in the near UV, visible and near IR were carried out by many researchers in two types of measurements; spectral global solar irradiance and broadband solar irradiance. The results from this study show that the measurement of the spectral solar radiation in the near UV, visible and near IR ranges can be made either by high precision and expensive instruments or by aid of rather simple, less precise and comparatively inexpensive broadband instrument—pyrheliometers or pyranometers in combination with glass filters. Selected narrow waveband instruments are characterized by simpler, less expensive and easy to maintain and calibrate compared to high-resolution scanning instruments.

Contents

1. Introduction

The intensity of solar radiation varies with the wavelength of the radiation, and the functional relationship between intensity and wavelength is called the solar spectral distribution. The spectral distribution of solar radiation outside the earth's atmosphere, called the extraterrestrial or air mass zero (AMO) spectrum, is well characterized. It roughly resembles the spectrum of a blackbody at 5900 K (Hulstron [1]) with a peak of the spectrum at a wavelength of about 500 nm (Webster [2]) and the exception of absorption lines caused by attenuation of radiation in the medium surrounding the sun (Hulstron [1]). This distribution is very important in solar applications such as the photovoltaic power systems of satellites, because their performances are spectrally dependent.

* Corresponding author.
E-mail address: y.a.eltbaakh@gmail.com (Y.A. Eltbaakh).

1364-0321/$ – see front matter © 2010 Elsevier Ltd. All rights reserved.
doi:10.1016/j.rser.2010.10.018

A knowledge of this distribution provides a design input for the better thermal environment of a spacecraft and for the selection of suitable materials exposed to solar radiation (Igbal [3]). When this solar radiation passes through the earth's atmosphere, the spectral distribution is modified by absorption and scattering of the radiation by atmospheric constituents, such as aerosols, ozone, and water-vapor. The exact spectral distribution at the earth's surface at any time depends on local atmospheric conditions and the path length of solar radiation through the atmosphere (or air mass). Air mass depends on the sun angle, which varies with location, time of day, and day of year (Hulstron [1]).

The electromagnetic radiation coming from the sun and reaching the earth's surface can be measured as broadband or total, spectral, or monochromatic. Total measurements include the whole range of wavelengths or the whole of corresponding energies, while spectral or monochromatic measurements are associated with a specific unit of wavelength. Total global irradiance which can be denoted by H and whose unit is $W\,m^{-2}$ is the solar hemispheric irradiance arriving at any point on the earth's surface. Monochromatic global irradiance is denoted by H_{λ}, its units are $W\,m^{-2}\,\mu m$ or $mW\,m^{-2}\,nm$, and it is the hemispheric irradiance corresponding to a narrow band of wavelength, as narrow as possibly measurable (for example: 1 nm, 0.5 nm, 0.1 nm, etc.). In general, both solar and spectral systems consist of a receiver, a detector, a signal or detector response processor and a counting system. The receiver makes it possible to receive radiation and to transfer it to the detector. The detector makes it possible to convert the solar energy, directly or indirectly, into an electrical signal (Pinedo et al. [4]). The objective of the present study can be broadly classified into threefold research effort; first effort is concerned with the measuring spectral global solar irradiance from the ultraviolet to the near infrared. Second, is interested in the measuring broadband global solar irradiance at the same region of wavelengths. The last one covers the methods that used to measure the extraterrestrial solar radiation.

2. Measuring broadband solar irradiance

Broadband instruments measure the combined solar intensity (irradiance) at all wavelengths (Pecht [5]). The instrument must be uniformly sensitive to all wavelengths from the very energetic and short wavelength X-rays to the very longest infrared wavelength (Calisesi et al. [6]). The most commonly used instruments to measure solar radiation today are based on either the thermoelectric or the photoelectric effects. The thermoelectric effect is achieved using thermopile that comprises collections of thermo couples, which consist of dissimilar metals mechanically joined together (Ghassemi [7]). The photoelectric effect is simpler and has instantaneous response and good overall stability. Among the photoelectric devices, photovoltaic instruments (PV) are most numerous in the field of solar radiation measurement. A photovoltaic device is made of a semiconducting material such as silicon (Igbal [3]). Instruments used to measure the transmission of sunlight through earth's atmosphere fall two general categories (Ghassemi [7]):

1. Pyrheliometers: these are instruments that measure direct radiation. Instruments measuring direct radiation usually include radiation coming out to an angle of about 3° away from the sun's disk. The sensor is a temperature-compensated thermopile placed at the bottom of a blackened collimator tube that limits the angular acceptance of solar radiation to about 5–6° (total). The instrument is oriented such that the direct radiation from the sun is parallel to the axis of the collimator tube.
2. Pyranometers: these are instruments that measure global and diffuse radiation. They have a shading disk to prevent direct solar radiation from reaching the sensor. The measurement for diffuse radiation involves correcting for the portion of the radiation shielded from the sensor by the shading disk. The sensor is a thermopile with alternate blackened junctions heated by the sun. The unheated junctions are near ambient temperature, which may be ensured by putting the unheated junctions in thermal contact with a white surface, heating by the sun is accomplished by placing the junctions in contact with a black surface (with high thermal conductivity) or by placing a black coating on the junctions. The instrument is installed in a level position, the sensor facing up towards the sky. Less expensive pyranometers may use a photovoltaic sensor to measure solar radiation (Pecht [5]).

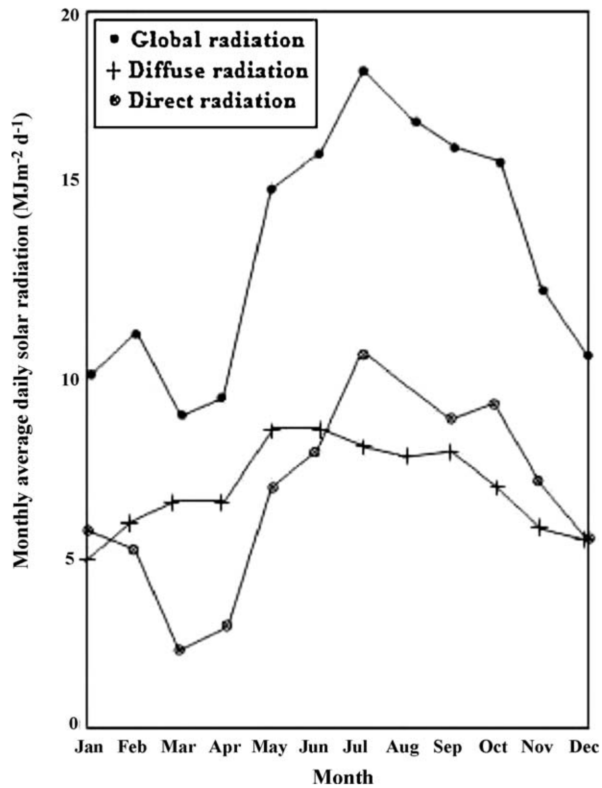


Fig. 1. Monthly average of daily global, diffuse and direct solar radiation (Lam and Li [8]).

2.1. Total broadband solar irradiance measurement

Lam and Li [8] measured both hourly horizontal global and diffuse solar components at City Polytechnic of Hong Kong during the 3-year period from 1991 to 1993 by using two pyranometers (CM11), manufactured by Kipp and Zonen. The diffuse radiation pyranometer was fitted with shadow-ring (CM121) to shade the thermopile from the direct sun. The pyranometers connected to an integrator (CM12) to calculate radiation over selected periods. A Pascal program had been written to capture the data from the integrator and store the data on a micro-computer. The monthly average of daily global, diffuse and direct solar radiations on a horizontal surface are shown in Fig. 1. The results showed that the annual average of global, diffuse and direct radiation were 13.4, 6.8 and 6.6 $MJ\,m^{-2}\,d^{-1}$ respectively. Solar radiation during the day lends to be more evenly distribution in summer than in winter, and the maximum hourly value occurred at solar noon for both global and diffuse radiation.

Jacovides et al. [9] used several measured wavebands, 300–630 nm, 300–710 nm and 300–2800 nm which was measured using the Linke–Feussner pyrheliometric in Athens, Greece for the period 1954–1990 to study the effects of aerosol on the direct

beam spectral solar irradiance distribution through effective optical depths. The observations were made at the National Observatory of Athens (NOA: latitude = 37°58′, longitude = 23°43′E, height above sea level = 107 m), at 11:20 and 14:20, Local Standard Time (LST is 2 h ahead of UTC) were used whenever clouds did not obscure the sun. Approximately seven thousand observations of direct solar spectra (300–710 nm) were taken under clear sky conditions defined to be less than 1/8 cloud cover with no clouds near the sun disk. Effective optical depths in the wavebands 300–630 nm, 300–710 nm and 300–2800 nm were calculated using Eqs. (1)–(3) respectively

$$\tau_t = \frac{[\ln I_t^* - \ln I_t]}{m} \quad (1)$$

where $I_t^* = I_{\Delta\lambda}^*$ and $I_t = I_{\Delta\lambda}$ are the direct beam irradiances for an aerosol free and a real atmosphere, respectively, for the whole spectrum 300–2800 nm.

$$\tau_t = \frac{[\ln I_r^* - \ln I_r]}{m} \quad (2)$$

where $I_r^* = I_{(300-630\,\text{nm})}^*$ and $I_r = I_{(300-630\,\text{nm})}$ are the corresponding direct beam irradiances for the finite waveband 300–630 nm.

$$\tau_\nu = \frac{[\ln I_\nu^* - \ln I_\nu]}{m} \quad (3)$$

where $I_\nu^* = I_{(300-710\,\text{nm})}^*$ and $I_\nu = I_{(300-710\,\text{nm})}$ are the corresponding direct beam irradiances for the finite waveband.

Fig. 2 shows the variation in mean monthly values of effective optical depths τ_r, τ_ν and τ_t and their standard deviations (SD) for the Athens Basin.

1 The relationships between τ_r and τ_ν, and τ_t and τ_ν were found to be linear.
2 Both spectrally resolved optical depths τ_r and τ_ν increase from 1954 until approximately 1975 and thereafter decrease gradually. τ_t optical depth increases during the period 1954–1977 and from 1985 decreases slightly towards the end of the period. During the early period 1954–1961 and during 1985–1990 the mean monthly values of both spectrally resolved optical depths coincide.
3 The results showed that there may be a considerable depletion of direct beam solar irradiance because of the effective attenuation by atmospheric aerosol. In addition, the spectral distribution of direct irradiance in the visible waveband may also be significantly altered as attenuation by scattering increases markedly towards shorter.
4 The effect of increasing aerosol concentrations on the visible band in the direct solar beam was investigated indirectly through the spectrally resolved optical depth τ_ν. It was shown that the direct solar beam in the waveband 300–700 nm was markedly depleted.

Singh et al. [10] measured the global solar radiation on a horizontal surface at Lucknow (latitude 26.75°N, longitude: 80.50°E, altitude 120 m above sea level), Uttar Pradesh, India from April 1991 to March 1992 by using a precision pyranometer (calibration constant: 5.5 mV cal^{-1} cm^{-2} min^{-1}). A potentiometric chart (0–10 mV, a chart width of 120 mm and a normal chart speed of 20 mm h^{-1}) recorder used to record the output of the pyranometer. These data had been analysed to develop new regression constants for estimating the hourly global solar radiation on a horizontal surface, which is based on the solar model proposed by Al-Sadah et al. Verification of the present constants was made by comparing the estimated ratios of hourly to daily global radiation (I/H) with the measured values. The estimated values of the monthly mean ratios (r/R), along with the measured values, as a function of the local time t for all the months of the year were plotted. Two samples have been chosen to be presented in this review (see Fig. 3). The results showed that the hourly global solar radiation on a horizontal surface can be satisfactorily estimated for the plane areas of Uttar Pradesh, India by using the new regression constants.

Souza et al. [11] used a Kipp and Zonen pyranometer, model CM5, to measure global solar radiation over the area of Maceió (9°40′S, 35°42′W, 127 m), located in Northeastern state of Alagoas, Brazil, during the period of January 1997–December 1999. The instrument connected to a data acquisition system, Micrologger 21XL Campbell Scientific Inc. which was programmed to yield information every 10 s and store averages value every 5 min. On cloudy days ($K_t^d \leq 0.03$) during the dry season and rainy period

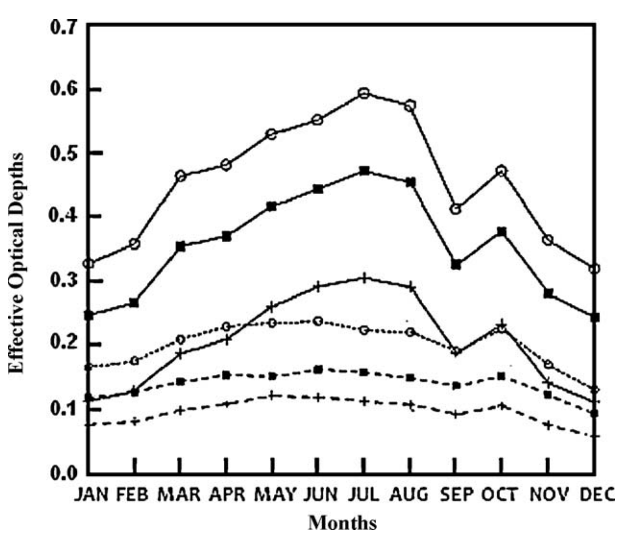


Fig. 2. Monthly mean values of effective optical depths τ_r, τ_ν and τ_t and their standard deviations for Athens basin (Jacovides et al. [9]).

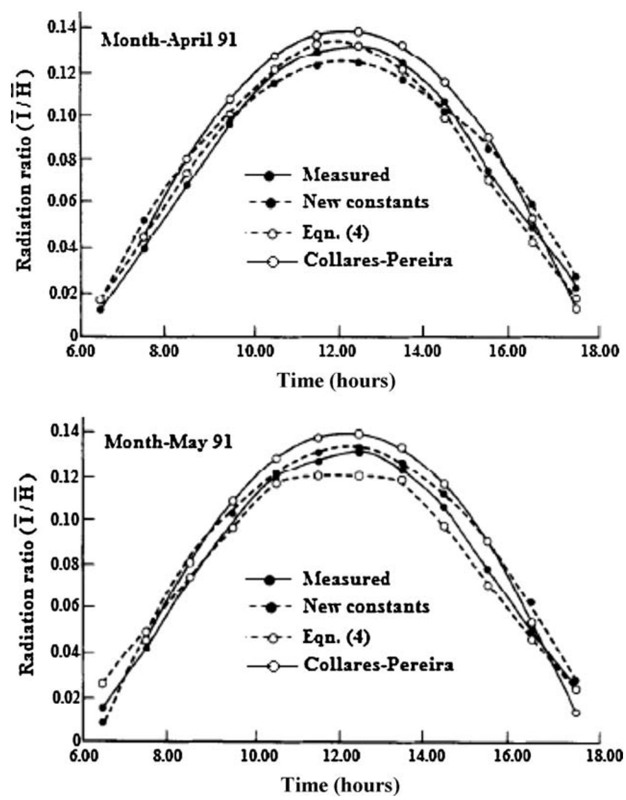


Fig. 3. Measured and estimated ratios of monthly mean hourly to daily global radiation for the months of April and December 1991 (Singh et al. [10]).

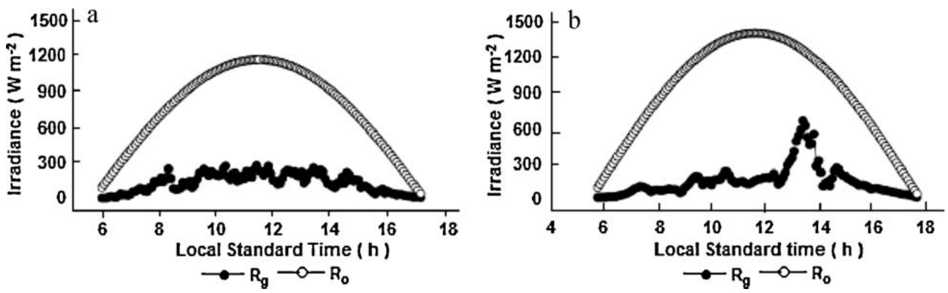


Fig. 4. Daily variations of extraterrestrial solar irradiance on a horizontal surface (R_o) and global (R_g), for (a) 07.26.1998 and (b) 02.18.1997, in Maceió, under overcast sky conditions (Souza et al. [11]).

(Fig. 4a and b) they were observed. The results showed that the maximum value of the hourly global solar radiation in the dry (September–February) and rainy (March–August) seasons were 3.18 and 2.5 MJ m^{-2}, respectively.

Islam et al. [12] measured the global solar radiation at the Petroleum Institute of the capital city of the UAE, Abu Dhabi (24.43°N, 54.45°E) for one complete year 2007 with Middleton Solar EQ08-E First Class pyranometer; its calibration accuracy is ±3%, its short wave sensitivity is 1.00 mV W^{-1} m^{-2} and its response time (95%) is 11.7 s to get a better view of the solar energy potential in Abu Dhabi. Fig. 5 describes the daily average and daily maximum global solar radiation for the whole year of 2007. Daily average solar radiation data showed that average values were higher in the summer from April to August and were comparatively lower in winter. The highest daily average solar radiation value of 369 W m^{-2} was measured on May 3, whereas the daily maximum global radiation of 1041 W m^{-2} was recorded on February 8. Average daily energy throughout the year 2007 was 18.48 MJ m^{-2} day^{-1}.

Islam et al. [13] measured the direct solar radiation at the Petroleum Institute of the capital city of the UAE, Abu Dhabi (24.43°N, 54.45°E) with Middleton Solar DN5-E pyroheliometer in 2007 for a complete year. The instrument was set 15 m from the ground level and recorded the direct solar radiation each 1 min. Daily and monthly of direct solar radiation were calculated from the one-minute average recorded by a Middleton Solar DN5-E pyranometer. Fig. 6 displays daily averages and daily peaks of direct beam solar radiation throughout the year. The results shows that the daily 1-min average maximum radiation of 937 W m^{-2} was recorded on February 20 whereas the highest daily average direct solar radiation value of 730 W m^{-2} was recorded on March 30, 2007.

2.2. Ultraviolet broadband solar irradiance measurement

Ogunjobi and Kim [14] made a series of measurements included ultraviolet UVB (280–320 nm), UVA (320–400 nm), broadband global (H_G), and diffuse (H_D) horizontal solar radiation continuously recorded from June 1998 to August 2001 at the Department of Environmental Science Building, Kwangju Institute of Science and Technology (lat. 35°10′N, long, 126°53′E, altitude 90 m asl), South Korea. The Kipp and Zonen model CM-11 pyranometers used to measure global solar irradiance and a second Kipp and Zonen model CM11, with a polar axis shadow band used to measure solar diffuse irradiance. The shadow band of the instrument blocks a strip of sky with a 3.3° umbral angle. The UV-S-B-T and UV-S-A-T pyranometers from Scintec were used to measure total irradiance from 280 to 320 nm and from 320 to 400 nm, respectively. The manufacturer indicates an accuracy of 10% for observation made for zenith angles between 0 and 50°, 6% between 50° and 60°, and 8% between 60j and 70°. The UVA and UVB radiometers present a cosine effect that is better than 5% for 0–60° zenith angles. Results from statistical analysis indicated that the minimum values were not representative of the total UV irradiation (HUVT) characteristics in Kwangju and, as such, they must be treated as being atypical. However, it may be concluded that the maximum values varying between 65.4 and 158.9 kJ m^{-2} can be considered as being representative of the hourly HUVT radiation at Kwangju. The monthly average hourly ratio of HUVT to HG varies from 7.0% to 9.4%. The highest value of HUVT accumulated throughout the year was observed in August, while the minimum was in January.

Jacovides et al. [15] measured the hourly global UV (G_{UV}) (UVB and UVA), global (G_h) and diffuse (G_d) solar irradiances at the semi-urban Athalassa site, Cyprus (35°15′N, 33°40′E, 165 m above MSL) in the eastern Mediterranean basin, during an ongoing joint research campaign (1 January–31 December 2004) between the University of Athens (Laboratory of Meteorology) and the Meteorological Service of Cyprus, to determine the ratio of solar global UV to solar global irradiation (G_{UV}/G_h) and its dependence on various atmospheric conditions. Solar global irradiance (305–2800 nm) was measured using the Kipp & Zonen model CM11 pyranometer (Delft, The Netherlands); a second Kipp & Zonen model CM11 with a polar axis shadow-band was used to measure the diffuse component. Solar global UVB and UVA components were measured with Skye High-Output Sensors (SKU-430 and 420, respectively, Skye, Powys, UK). Both instruments used a photovoltaic sensor in

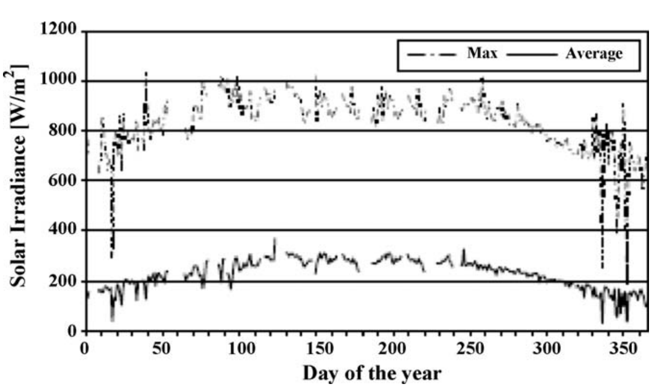


Fig. 5. Daily averages and daily peaks of global solar radiations throughout the year (Islam et al. [12]).

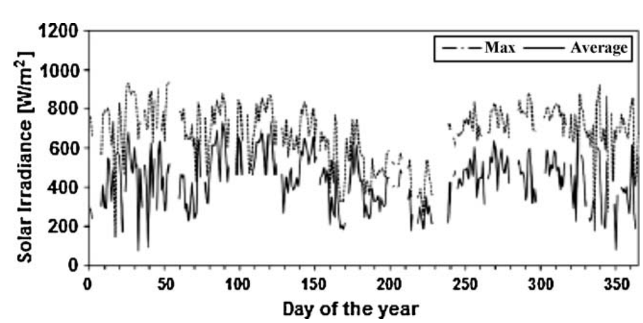


Fig. 6. Daily averages and daily peaks of direct beam solar radiation throughout the year (Islam et al. [13]).

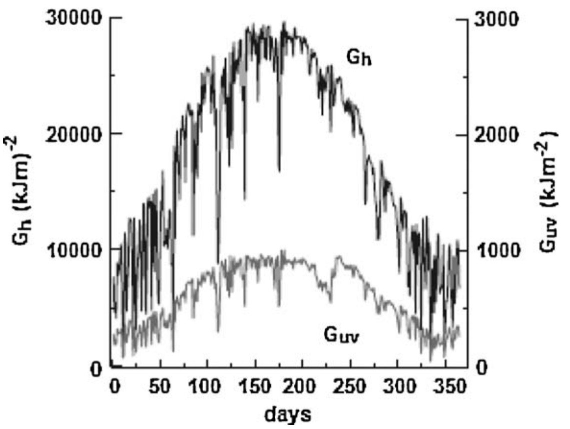


Fig. 7. Annual pattern of daily solar global UV and solar global irradiation values, for Athalassa, Cyprus (Jacovides et al. [15]).

combination with special filters to detect the wavelengths they are designed for. The Skye sensors are calibrated in accordance with UK national standards via the National Physical Laboratory (NPL). Fig. 7 shows the daily variability of both radiant fluxes, G_h and G_{uv}, for the period of measurements.

The results showed that the percentage ratio G_{uv}/G_h ranges from 3.9570.29% in September to 2.9270.42% in August for hourly values, while for daily values, the ratio varies between 3.6870.1% in September and 2.8570.32% in August, with annual mean value of 3.1970.17% for daily ratios and up to 3.3370.21% for hourly values. The hourly and daily values of both radiant fluxes are highly correlated with a general linear relationship of the form $G_{uv} = \alpha G_h$ between the measured values providing coefficients of determination R^2 always greater than 0.91 for hourly and 0.88 for daily fittings.

3. Measuring spectral global solar irradiance

The increase in terrestrial applications of solar radiant energy in different disciplines such as climate studies, atmospheric physics, photovoltaic cells for electrical generation and selective absorbers for thermal collectors and for practical applications in environmental and agro meteorological research, has given impetus to study the solar energy availability in Malaysia. Spectral selective devices share their interest in the accurate knowledge is not in the total (integrated over all wavelengths, also called broadband) amount of solar energy reaching the earth's surface, but also in its spectral composition.

3.1. Visible and near-infrared

3.1.1. Overview

Over 99% of the energy flux from the sun is in the spectral region of 150–4000 nm (Godish [16]), with approximately 41% in the visible region and 51% in the infrared region (Mora et al. [17]). The visible region of the spectrum is flanked by ultraviolet (above violet in terms of frequency) and infrared (below red) regions. The near infrared portion which extended from the boundary of the visible up to 4000 nm, is dominated by solar radiation, whereas the remainder of the infrared region is dominated by terrestrial (i.e. earth emitted radiation: hence, the near infrared region is included in the term shortwave radiation (Godish [16]). The solar radiation at wavelengths between 300 and 10,000 nm is of special interest for both solar physics and climatology for the following reasons: Firstly, most of the solar radiative output (99%) occurs at these wavelengths. Hitting the earth, radiation from this part of the spectrum that is not scattered back into space by the earth's atmosphere, clouds and the surface is absorbed in the biosphere, the surface and the oceans where it, hence, directly determines the thermal energy balance of the earth's atmosphere. Secondly, this part of the spectrum, formed mostly deep down in the solar photosphere, holds the key to unraveling the relation between solar surface (magnetic) features and total or spectral solar irradiance changes (Fligge et al. [18]).

3.1.2. Detection system

The instrumentation for the measurement of solar spectral energy distribution as a function of wavelength is more complex and varied than total irradiance measurements. Monochromators with a wavelength range of 290–3000 nm with integrating sphere attachments are employed where high wavelength resolution is required. For most purpose broad band spectral energy distribution data is sufficient. Interference filters which transmit the energy over a known spectral band or glass cut off filters which transmit all wavelengths beyond a known limit are used in combination with a total irradiance detector like a pyranometer. The wavelength resolution is 10–100 times less than for a monochromator. The Eppley spectral pyranometer with 6 filter hemispheres as outer domes is often used for these broad band spectral energy measurements (Lim [19]).

3.1.2.1. Selected wavelengths spectral solar radiation measurements. A sun photometer is an instrument used to measure solar radiation at selected wavelengths. This instrument is usually constructed with a limited FOV, interference filters, and detectors. Sun photometers measure the radiation from the sun within the bandwidth of the optical filter. Typical filter bandwidths are 5–10 nm at half-maximum, and the FOV is usually less than 3°. Measurements at selected wavelengths can be used to calculate the total optical depth of the atmosphere at these wavelengths. For this purpose, the World Meteorological Organization recommends that the central wavelengths of the filters be at 368 nm, 500 nm, 778 nm, and 860 nm. Sun photometers can be calibrated in the laboratory, but most of the calibrations are performed outdoors using the Langley plot method (Hulstron [1]).

Wehrli and Frohlich [20] used a sunphotometer (SPM05) to measure the solar irradiance at three wavelengths 368 nm, 500 nm and 778 nm from rockets and a balloon over a period of three years between 1983 and 1986. The sunphotometer was developed at the Physikalisch-Meteorologisches Observatorium Davos (PMOD) and calibrated by an irradiance standard lamp. The sunphotometer has three independent channels with filtered silicon detectors and electronics in a tubular housing of 5 cm diameter and length 30 cm. Each channel consists of an interference filter placed between a precision aperture of 2, 0 mm nominal diameter and a EG&G UV215 photodiode. The field of view is restricted by a field aperture of 4, 3 mm at a distance of 98 mm from the detector aperture to 1.3° full cone angle. The electronic circuit as shown in Fig. 8 consists of a low noise current to voltage converter followed by a voltage amplifier for a full-scale reading of nominally 10 V.

The SPM05 was flown together with two absolute radiometers three times in December 1983, 1984 and 1986 on a rocket about 300 km and once on a stratospheric balloon in June 1983 from White Sands (New Mexico). Analogue to digital conversion was carried out by two voltages to frequency converters with 100 ms integration time and 15 bits resolution. About 900 samples were taken for each SPM channel while pointing at the sun, and several hundred additional samples measured zero points while looking into deep space. The stratospheric balloon experiments Solar Irradiance Monitoring from Balloons (SIMBA) had also been flown since June 1983. SIMBA had also been launched in Aire-sur-1'Adour (France) on 28 September 1985. Sunphotometer measurements were taken during 1 h, while the balloon floated at 3.3 hPa (40 km).

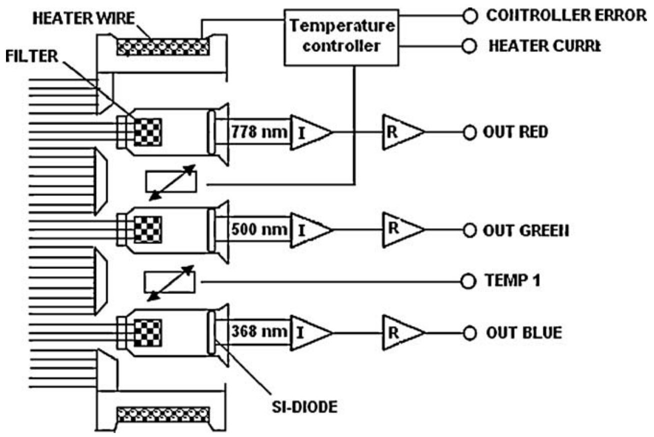


Fig. 8. Block diagram of sunphotometer SPM05 (Wehrli and Frohlich [20]).

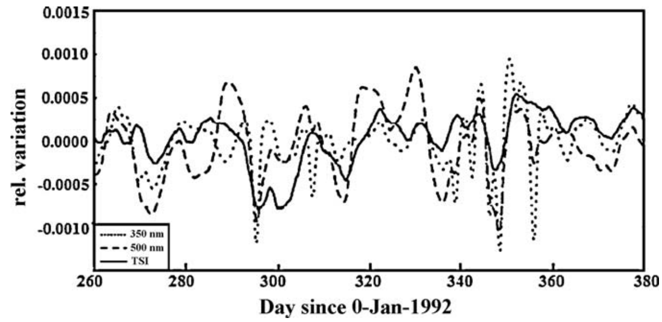


Fig. 9. Relative residuals of SPM red and green channel after cubic spline fit through averages over 123 segment means and smoothing by triangular running mean. Solid line shows relative variations of total solar irradiance measured by SOVA2 absolute radiometer (Wehrli et al. [21]).

The results showed the blue channel changes far more than the red or green channels. The red and blue values for the SIMBA85 experiment seem to be markedly different from the rocket values, but not so the green one.

Wehrli et al. [21] measured the solar irradiance at 3 wavelengths (335, 500 and 862 nm) by the expaiment SOVA2 on the European Retrievable Carrier (EURECA). SOVA2 built by the Physikalisch-Meteorologisches Observatorium Davos (PMOD) with two absolute radiometers, a high resolution, relative radiometer, two sunphotometem, SPM, with 3 channels (blue, red and green) and a sun-pointing sensor. Sunpbotometer is a three channel spectral radiometer using silicon detectors and interference fibers centred at 335, 500 and 862 nm with a bandwidth of 5 nm.

The primary instrument SPM-A experienced strong degradation in all 3 channels while SPM-B, which was exposed for less than 1% of the possible time, degraded much less. The degradation did not occur as a smooth function of time but shows variable rates that increased after the cooling loop was switched off. No detailed knowledge about the degradation process is available and simple analytical function like an exponential or polynomial in time produce residuals that bear no resemblance to the measured total solar irradiance variations. Cubic spline functions fitted through averages over N segment means were used instead, where N is a free parameter. Large values of N, approximating the degradation globally, produce residuals similar to a polynomial fit. Small values of N, treating degradation more locally, result in smaller residues with occasional, sharp oscillations typical for overshooting splines. Fig. 9 shows the residuals of the 500 and 862 nm channels for a fit with $N = 123$, corresponding to averages over 8 days, together with the variation of the total solar irradiance measured by the absolute radiometer PMO6 of SOVA2.

Rabbette and Pilewskie [22] used principal component analysis (PCA) technique to characterize approximately 7000 down welling solar irradiance spectra retrieved over the duration of the experiment, between September 17 and October 4, 1997 in atmospheric conditions that varied from pristine clear to very thick cloud cover, accompanied by a fivefold change in column-integrated water vapor (1–5 cm) at the Southern Great Plains site. The statistical technique PCA is applied to a set of variables with the aim of finding subsets of variables which are independent of other variable subsets. The PCA is a method of transforming the original variables into fewer uncorrelated variables.

The basic steps employed in the PCA procedure were as follow:

1. An input data set is acquired by repeated measurements of a selected set of original variables (solar irradiance at various wavelengths).
2. A variable correlation matrix is constructed from the time series of spectra.
3. The principal components (PCs) (the term given to a subset of variables highly correlated with each other but relatively independent of the remaining subsets of Variables) are extracted from the correlation matrix.
4. APC rotation is applied to improve the interpretability of the solution.

Each (PC) has a corresponding time series. The time series of a rotated principal component can be calculated from the following matrices: (1) the original variable matrix (i.e. irradiance at various wavelengths); (2) the component rotation or transformation matrix (T); (3) the unrotated principal component matrix (P). Fig. 10a and b shows one of the first six principal components

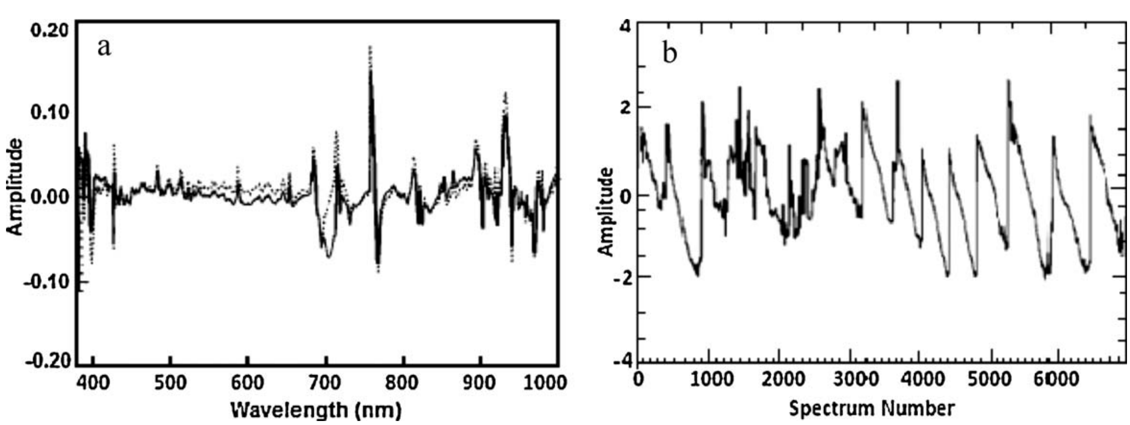


Fig. 10. (a) The first principal components of the SSFR data array (solid lines, unrotated components dotted lines, rotated components). (b) Time series plot for first rotated components (Rabbette and Pilewskie [22]).

extracted from the visible SSFR array and the time series plot corresponding to it.

The results from the visible array, 380 nm to1000 nm were:

1. By applying PCA to SSFR spectra the variability in solar spectral flux due to fundamental atmospheric parameters such as liquid water content, water vapor, molecular scattering, and ozone absorption had been quantified.
2. PCA also facilitates tremendous data reduction.

3.1.2.2. Broadband spectral solar radiation measurements. Solar radiation measurements devices equipped with special filters can be used to measure solar radiation in relatively broad portions of the spectrum for particular applications. For example, filters that select a portion of the spectrum from 400 nm to 700 nm are used to measure solar radiation in the photosynthetically active region of the spectrum for plant studies. Another example is a sensor with a spectral responsivity curve equal to the response of average human eye (photopic response). This sensor can be used for studies that require illuminance data, such as building system studies on day lighting (Hulstron [1]).

Laue [23] used multichannel radiometers to establish the solar constant and its spectral components at an elevation of 1.3 and 2.3 km (Table Mountain, California). The multichannel radiometers were composed of three-channel bandpass system monitoring the total, ultraviolet and infrared irradiances, and using wire wound-plated thermopiles blackened to eliminate spectral selectivity. The experiment involved inter-comparing two multichannel radiometers at Table Mountain (TM) at 2.3 km elevation, and then transporting one of the radiometers to the JPL Edwards Test Station site (ETS), 60 mi north and at 1.3 km elevation. Concurrent observations at the two sites were made throughout the succeeding day to illustrate the spectral attenuation effects. All of the data were obtained under as nearly ideal, clear-sky conditions as possible. The comparative values of the total irradiance throughout one day at both test sites are shown in Fig. 11.

Michalsky and Kleckner [24] applied two mathematical techniques (WIENER and PARK-HU) for estimating continuous direct solar spectrum for given atmospheric conditions using the SOLTRAN5 based on seven broad-band filter measurements between 360 and 1030 nm. On 1 July 1981, eight sets of filter measurements were collected in a period of one and one-half hours centered on 12:49 local time. The total irradiance as monitored by the companion pyrheliometer varied between 954 and 966 W m^{-2} during that period. The eight seven-filter sets were averaged to produce seven values which yielded the estimated spectrum of Fig. 12a. Spectral distribution of direct solar radiation had been calculated (see Fig. 12b) using SOLTRAN5 which is the transmission calculated from LOWTRAN5 multiplied by the extraterrestrial spectrum according to the prescription of (Bird and Hulstrom 1983).

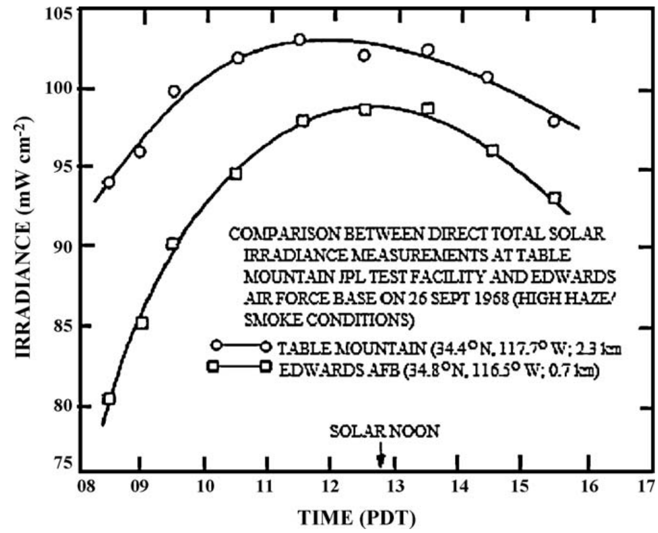


Fig. 11. Total irradiance intercomparison; Table Mountain (TM) and Edwards Test Station (ETS) (Laue [23]).

The estimation procedure had been applied to a set of "measurements" generated by convolving the SOLTRAN5 spectrum with the actual filter transmission functions. The estimated spectrum which results from this procedure is given in Fig. 13a and b along with the SOLTRAN5 spectrum.

Either the Wiener or the Park–Huck estimation procedure provided a satisfactory method of estimating spectra from filter data. Except for the end points, which can be adjusted according to the assumptions at these boundaries, there was less than a two per cent difference, and most often less than a one per cent difference, throughout the spectrum. The difference in the estimates was near a minimum at the central wavelengths of the middle five filters.

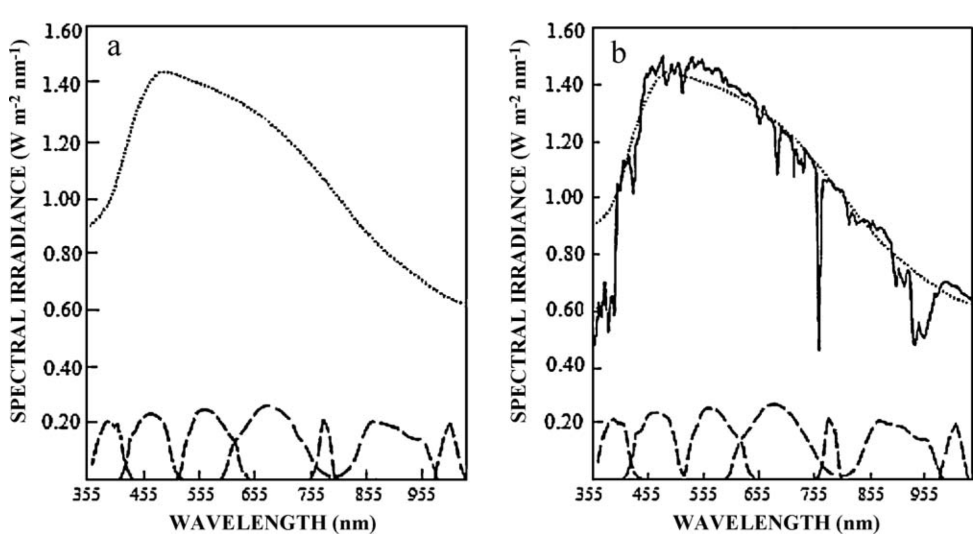


Fig. 12. (a) Wiener estimated spectrum of near-noon direct solar spectral irradiance based on measurements through indicated filters. (b) Estimated spectrum from (a) and SOLTRAN5 direct solar spectrum calculated for time of measurements (Michalsky and Kleckner [24]).

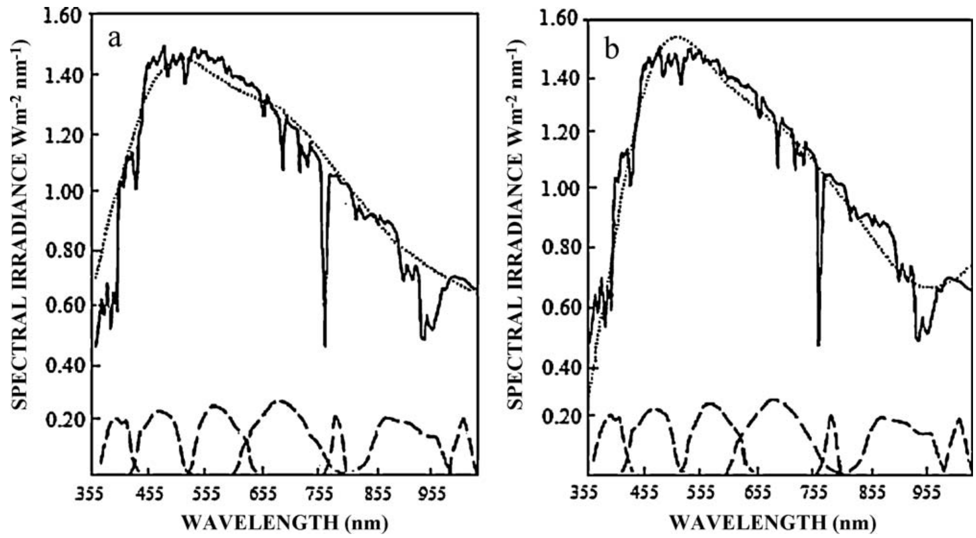


Fig. 13. (a) SOLTRAN5 spectrum from Fig. 2 and Wiener estimated spectrum resulting from measurement simulation based on convolution of SOLTRAN5 spectrum and filter. (b) Same as (a) except Park–Huck estimated spectrum (Michalsky and Kleckner [24]).

Michalsky [25] continued to compare spectral irradiances to substantiate the reliability and applicability of estimated spectra based on filter measurements using actual data. Theoretical spectra had been generated using a model developed by (Bird, 1984) (hereafter, SPECTRAL). Estimated spectra from filter measurements were compared to modeled data based on the independently measured aerosol and water vapor content of the atmosphere, and the solar geometry during the measurement. Estimated spectra were also compared to absolutely calibrated spectroradiometric measurements. Insolation measurements had been made on 1 July 1981, with an active cavity radiometer (ACR) to measure the irradiance through each of seven filters held in the beam of the radiation incident on the ACR near solar noon (at a minimum air mass) and repeated the complete set of seven as often as possible so as to improve the signal-to-noise ratio.

Estimated spectra from filter measurements were compared to modeled data based on the independently measured aerosol and water vapor content of the atmosphere, and the solar geometry during the measurement. The average for each of the seven filters was used as input to the Wiener estimation procedure. The resulting spectrum appears superposed on the SPECTRAL model spectrum in Fig. 14.

A further test of the validity of estimated spectra from filter data was made using simultaneous observations with an absolute spectroradiometer. Actually two series of measurements separated by 1.5 h had been made Fig. 15 displays one of the measurements, comparison of the Wiener estimate of the direct solar spectrum derived from filter measurements, the SPECTRAL modeled spectrum and spectroradiometric data taken with an absolutely calibrated instrument in May 1982.

The results presented in this paper highlight:

- The integrated spectroradiometric measurement was agreed to within 1%, but the detailed agreement throughout the spectrum is not quite as good as for the simulation.
- The integrated modeled data was 5% lower than the spectroradiometric data and the estimated data, but the results are within the stated error of 7% in the absolute spectroradiometry.
- Better agreement is spectral detail is demonstrated for simulated measurements by improving the filter selection.

King et al. [26] described straightforward methods for directly measuring the influences of variations in solar spectral irradiance and solar angle-of-incidence as a function of time-of-day on the characterization and array performance of photovoltaic module. A convenient method to account for the spectral influence had evolved from their outdoor testing experience coupled with standardized test methods (ASTM). Eq. (4) describes ASTM, providing a spectral mismatch parameter, M. The mismatch parameter was used to correct measured values of short-circuit current, obtained using an arbitrary test spectrum, to the value appropriate for one

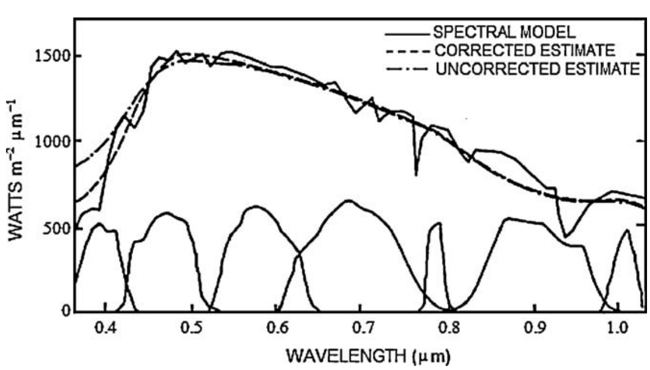


Fig. 14. Comparison of the Wiener estimate of the direct solar spectrum derived from filter measurements with an active cavity radiometer and the SPECTRAL modeled spectrum based on measured aerosols and estimated water vapor and ozone for July 1981 (Michalsky [25]).

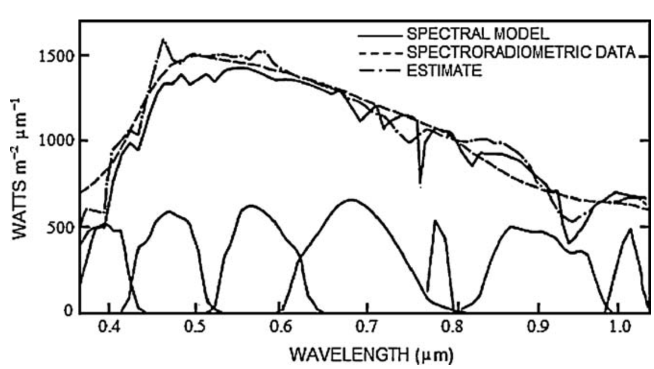


Fig. 15. Comparison of the Wiener estimate of the direct solar spectrum derived from filter measurements, the SPECTRAL modeled spectrum and spectroradiometric data taken with an absolutely calibrated instrument in May 1982 (Michalsky [25]).

of the standardized solar spectral distributions.

$$M = \frac{\int_a^b E(\lambda)R_t(\lambda)d\lambda}{\int_c^d E(\lambda)R_t(\lambda)d\lambda} \cdot \frac{\int_c^d E_o(\lambda)R_t(\lambda)d\lambda}{\int_a^b E_o(\lambda)R_t(\lambda)d\lambda} \qquad (4)$$

Since the spectral response of a typical thermopile pyranometer (Eppley PSP) can be considered to be essentially constant over its spectral response range (300–3000 nm). In this case, Eq. (4) reduces to the simpler expression given in Eq. (5).

$$M \approx \frac{I_{sc_t}}{E^*} \cdot \frac{E_o^*}{I_{sc_{to}}} = f_1(AM_a) \qquad (5)$$

The solar spectrum chosen as the reference for the test was the prevailing spectrum at the time of day when $AM_a = 1.5$. Therefore, E_o^* and Iscto were the values measured during this reference condition. In order to make the results independent of the day of the year, the spectral correction parameter was described as a function of AM_a. Fig. 16 illustrates the AM_a Functions measured for a variety of photovoltaic devices, including commercial crystalline, multicrystalline, and amorphous silicon modules, a Silicon-Film^{TM} module, and a siliconphotodiode pyranometer. The influence of solar angle-of-incidence on photovoltaic system performance had also been developed. The method used for calculating angle-of-incidence is given by

$$\mathrm{AOI} = \cos^{-1}\begin{bmatrix} \cos(T_m)\cos(Z_s) \\ \sin(T_m)\sin(Z_s)\cos(AZ_s - AZ_m) \end{bmatrix} \qquad (6)$$

The measurement procedure developed mprovided a second empirical function, f_2(AOI), called the "AOI Function" which related the module's Isc to the solar angle-of-incidence (AOI). The AOI Function addresses effects that are beyond the typical geometric "cosine" losses. During analysis, the measured Isc was translated to a reference solar spectrum using a previously determined AM_a Function, and to a reference temperature, T_o, using a temperature coefficient. Then, Eq. (7) gives the model used to calculate the AOI Function. Fig. 17 shows the measured AOI Functions for a typical flat-plate photovoltaic modules with a glass front surfaces, a silicon-photodiode pyranometer, and a typical Eppley PSP pyranometer:

$$f_2(\mathrm{AOI}) = \frac{I_{sc}(AM_a = 15, T = T_o) - C_2(E_E/1000)}{C_1(E_E/1000)\cos(\mathrm{AOI})} \qquad (7)$$

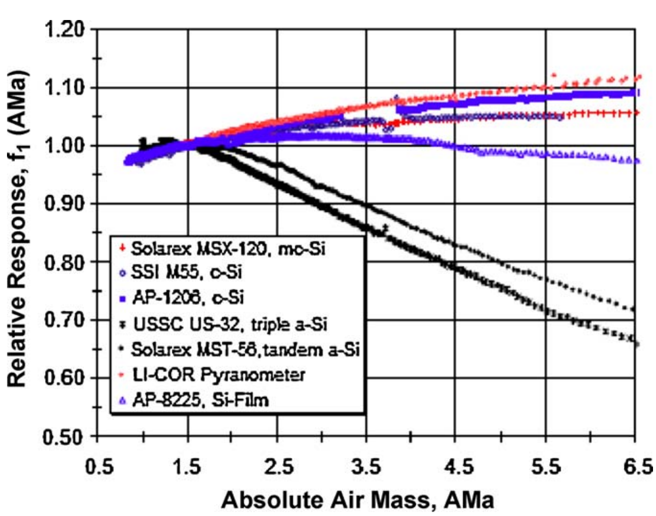


Fig. 16. Relative short-circuit current versus AM_a for a variety of photovoltaic modules and a silicon-photodiodepyranometer (King et al. [26]).

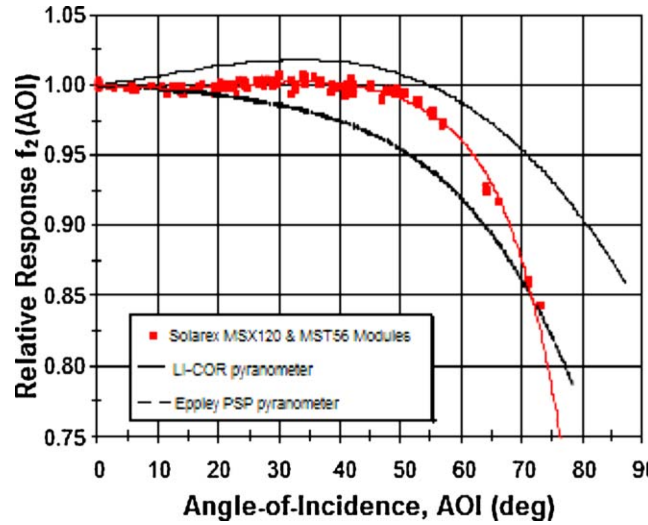


Fig. 17. Relative response versus AOI for a typical flatplate modules and two pyranometers. Results for the pyranometers [26] are shown as lines (King et al. [26]).

The results illustrated

- The benefit of relating the spectral effect to AM_a as the independent variable. In addition, the AM_a Function for modules under clear sky conditions had been found to be relatively consistent from day to day, season to season, and even site to site.
- The spectral distribution of direct solar irradiance changes significantly over the day, while the spectral distribution of diffuse solar irradiance remains nominally the same.
- For completely diffuse irradiance, module performance does not depend on solar angle-of-incidence; for instance, under very overcast conditions, I_{sc} does not change as the module is pointed in different directions.

3.1.2.3. High-resolution spectral solar radiation measurements. Relatively complex instruments (spectroradiometers) are available to make high-resolution spectral solar radiation measurements over a broad wavelength range. High-resolution spectral measurements are needed to study the fine structure in spectral distribution. It is important to record ancillary meteorological data, such as water vapor, with spectral measurements to isolate specific atmospheric effects on the spectra. One of the more sophisticated spectroradiometers was built under SERI's direction. This instrument can complete a spectral scan from 300 nm to 2500 nm with less than 1 nm resolution in 2.5 min. The instrument uses visible and infrared wavelength channels that simultaneously view an integrating sphere. The unique features of this instrument are continuous spectral solar radiation calibration, continuous wavelength calibration, continuous monitoring of broadband (300–1100 nm) solar radiation stability, and self-correction for changes in the response at each wavelength (Hulstron [1]).

Measurements of the solar spectral radiation in the visible and near-infrared ranges were carried out by many researchers. Stair [27] used spectroradiometer to measure the distribution of direct solar radiation in the range 209–535 nm for different air masses at Sunspot, New Mexico (altitude 9200 ft) in June 1955. The system was composed primarily of a Carl Leiss double quartz-prism spectrometer mounted on a polar axis driven by synchronous motor to follow (approximately) the path of the sun across the sky, and sector disk mounted on a synchronous motor to modulate the light beam. Also, a 935 emission-type phototube was employed as the detector in the ultraviolet and visible spectra to about 550 nm and strip recorder to register automatically the spectral data.

Table 1
Total solar irradiance measured, with Angstrom pyrheliometer, 27 February 1972 at Table Mountain, Calif. (Mecherikunnel and Duncan [28]).

Time	Total irradiance (W m^{-2})	Time	Total irradiance (W m^{-2})	Time	Total irradiance (W m^{-2})	Time	Total irradiance (W m^{-2})
10:15	1054	11:00	1056	11:45	1061	12:40	1056
10:20	1055	11:05	1050	11:50	1060	12:45	1050
10:25	1055	11:10	1054	11:55	1058	12:50	1056
10:30	1055	11:15	1053	12:00	1063	12:55	1054
10:35	1055	11:20	1054	12:15	1056	13:00	1043
10:40	1055	11:25	1055	12:20	1068	13:15	1043
10:45	1055	11:30	1055	12:25	1059		
10:50	1056	11:35	1058	12:30	1056		
10:55	1057	11:40	1061	12:35	1055		

Mecherikunnel and Duncan [28] presented the results of a series of total and spectral solar irradiance measurements made at ground surface (Table Mountain Facility, Calif., altitude 2.18 km). The spectral irradiance data were presented for the 300–3000 nm spectral region for air mass 1.5. Direct solar irradiance was measured with an Angström pyrheliometer mounted on a heliostat to track the sun. Solar spectral irradiance measurements were made with a Leiss quartz double-prism monochromator and a Perkin-Elmer LiF prism monochromator. The calibration of the monochromators was based on NBS quartz-iodine lamps. Most of the spectral scans were for the 300–1200 nm spectral region. But two spectral scans were made on both days for the 300–3000 nm spectral region with the Perkin-Elmer monochromator. The spectral irradiance was measured at 10 nm intervals except at the absorption bands, where closer intervals adequate for showing the width and depth of the bands had been chosen. The amount of precipitable water vapor during the observation time was 2 mm, very low compared to 19 mm, which is the average at sea level for midlatitudes.

The total irradiance observed remained fairly constant, ~1055 W m^{-2} throughout the observation of 27 Feb. 1972. Table 1 gives the total irradiance measured as a function of time. The direct solar spectral irradiance on Table Mountain measured for the 300–3000 nm spectral region based on the data of 27 Feb. 10:34 h, 1972 measured by the Perkin-Elmer and the Leiss for air mass 1.5, is presented in Fig. 18.

Thuillier et al. [29] used three separate spectrometers, which are double monochromators equipped with holographic con-cave gratings (f = 0.1 m) to measure and improve the absolute accuracy in the solar irradiance simultaneously in three channels: ultraviolet, visible, and infrared. The absolute solar radiation data were obtained by comparing the solar irradiance with the irradiance of an artificial light source for which the radiation is known in absolute units.

The sensitivity was controlled by two sets of lamps. Ten long-term standard (LTS) lamps were mounted in a special calibration

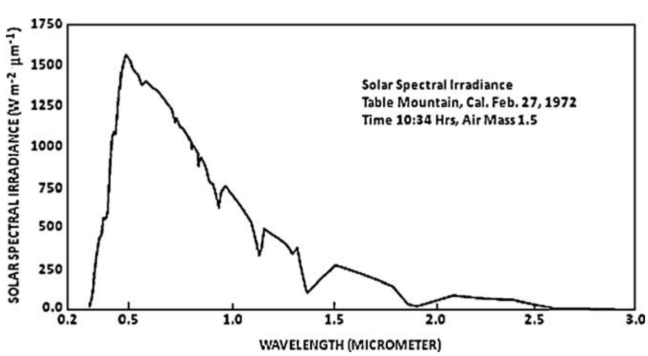


Fig. 18. Solar spectral irradiance for the 0.3–3.0-/tm spectral region, measured at ground surface, Table Mountain, Calif. [altitude 2.18 km (7200 ft)] on 27 Feb. 1972. Time 10:34 h. Solar zenith angle 48.20; air mass 1.5. Precipitable water vapor 2 mm (Mecherikunnel and Duncan [28]).

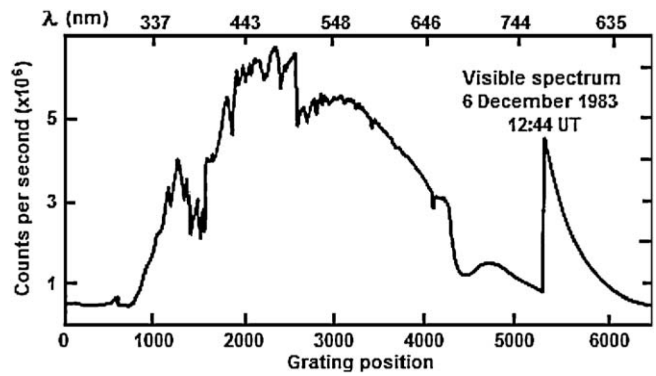


Fig. 19. (left) Ultraviolet spectrometer raw solar data.

unit, which can be fitted to the instrument as long as it is on ground (and accessible on the Spacelab pallet). The radiation from these lamps enters the spectrometers in the same way as the solar radiation. These LTS lamps make it possible to control the relative sensitivity of the spectrometers with high precision over time intervals on the order of several years. The second set of lamps consists of four in-flight calibration lamps (ICL's), which were mounted inside the instrument at fixed positions. Measurements of the ICL's and the hollow cathode lamp were made on days 1, 4, 8, and 9 of the Spacelab I mission. Solar spectra were recorded for 14 h on day 8. About one-third of the data were obtained in real time, one-third by playback; the rest of the data have not yet been delivered. The total number of solar spectra recorded in orbit was 35. A few of these spectra were excluded because during the observations the sun was viewed through the earth's atmosphere. Some examples of solar and lamp spectra are given in Figs. 19 and 20.

Cannon [30] used three spectroradiometers to cover the majority of the solar radiation spectral regime (i.e. 290–3000 nm). The "workhorse" of the three spectroradiometers was an instrument with a silicon-based detector and a single holographic grating:

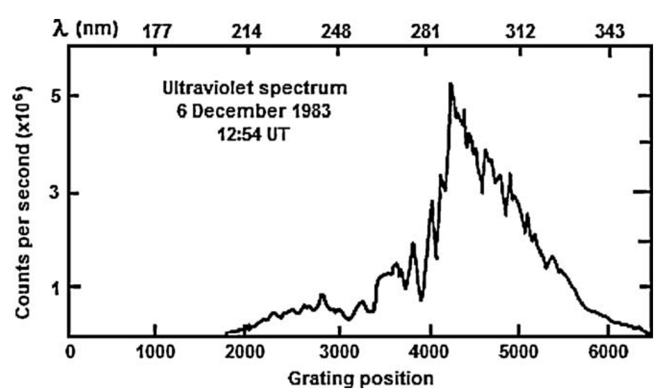


Fig. 20. (right) Visible spectrometer raw solar data (Thuillier [29]).

the LI-COR portable spectroradiometer (LSR) model LI-1800. It was used to measure the UV–VIS–near IR region (350–1100 nm). This instrument was used in virtually all of the measurements. The UV instrument was an ISA model DH-10 monochrometer with a Spectralink control and data acquisition unit. The Transportable Solar Spectral Radiometer (TSSR) spectroradiometer model 746D was used to cover IR region. TSSR was manufactured by Optronic Laboratories with a double monochrometer and a cooled lead sulfide detector to cover the 800–3000 nm range. This instrument can also be operated with a silicon detector to cover the 285–1100 nm regime.

In the case of the silicon-based LSR, temperature control was added to compensate for the temperature-dependent spectral response of the Si detectors, which can be as high as about 2% $^{\circ}C^{-1}$ at the most sensitive wavelength, 1100 nm. The UVSSR, LSR, and TSSR instruments all interface with HP-85 computers, selected because the storage media (tape), printer, display, and interface modules were all in one self-contained, portable unit. Programs for all three spectroradiometer systems were written so that the data files are formatted identically. In addition, programs were written which allow data from two or more instruments to be merged, ratioed or substracted.

Riordan [31] the Electric Power Research Institute (EPRI), the Florida Solar Energy Center (FSEC), and the Pacific Gas and Electric Company (PG&E) cooperated to build a spectral solar radiation database for a range of atmospheric conditions and air masses. Spectral solar radiation data as well as supporting broadband solar radiation and meteorological data were being collected at FSEC and PG&E and sent to SERI for processing and archiving. The spectral data were measured using LI-COR* Model LI-1800 spectroradiometers with holographic grating monochromators. Measurements are made from 300 to 1100 nm with a step size of 2 nm, a bandwidth of 6 nm, and a scan time of 26 s. Data were collected using several measurement modes that correspond to PV collector modes: direct-normal (concentrators); global-normal (two-axis tracking flat plates); and global-tilt (fixed-tilt or single-axis tracking flat plates). Global-horizontal data are collected to test models that convert radiation on a horizontal surface to radiation on a tilted surface.

Approximately 1300 spectra collected by FSEC and PG&E were processed through visual quality-control program and archived at SERI by October 1987. Figs. 21a, b and 10 show two examples of measured spectra from the database. These data show global-normal spectral solar radiation (tracking flat plate) measured from morning until noon on a partly cloudy to cloudy day in winter and on a relatively clear day in summer.

Manjul and Verma [32] carried out multitemporal measurements in ten discrete spectral bands in the range from 400 to 1000 nm with the help of indigenously developed Spectropolarimeter. The measurements had been carried out at Wheat Research Station, Vijapur, Mahesana under minimum haze sky conditions twice a week in a period of about 100 days to generate a data bank for a period from December 88 to April 89 and to be useful to interpolate the ground solar spectral irradiance at any time and any day in the same period. The station was far away from any industrial activity and was least affected by any atmospheric pollution. The field of view of the instrument was converted into 180° (circular) with the external attachment of the opal glass at the entrance aperture to measure direct as well as diffused component of solar radiant flux.

All measured values of spectral irradiance w.r.t. local time were entered and the data was processed with LOTUS 1–23. For every spectral band, the atmospheric transmittance values of all the days were normalized w.r.t. 8th and 9th April 1989 data which consisted of 40 measurement points. Typical measured spectral irradiances and estimated atmospheric transmittances were at sun zenith angle of 20° and 60°. Best fit curves with 2nd order polynomial equations were fitted into these points. The coefficients were obtained separately for east and west direction. Best fit curves of global solar spectral irradiance and estimated atmospheric transmittance w.r.t. sun angle are presented in Fig. 22a and b. The estimated atmospheric transmittances were compared with the AFGL LOWTRAN 6 atmospheric model 5.

The results of the study indicate:

1. Coefficients and normalization factors for every spectral band were useful to interpolate the ground solar spectral irradiance and atmospheric transmittance with the maximum experimental errors of 11%. The measurement data and interpolated data could be useful to support/verify theoretical models and practical measurements.
2. For the same zenith angle, the atmospheric transmittance was lower when the sun was towards west. The difference increases as zenith angle increases. The decrease in transmittance at 60° zenith angle was about 4%.
3. Even under relative cloud free conditions, multidate transmittance varied to about 25%.
4. In general, LOWTRAN values and estimated values of atmospheric transmittance were comparable.

Martinez et al. [33] used LI-COR 1800 portable spectroradiometer with a 6 nm bandwidth and controlled by a portable pc and the manufacturer's software and fitted with a silicon photodiode as a detector to measure global and diffuse solar irradiance on a horizontal plane and global, direct and diffuse solar irradiance on a plane normal to direct solar radiation in the range 300–1100 nm

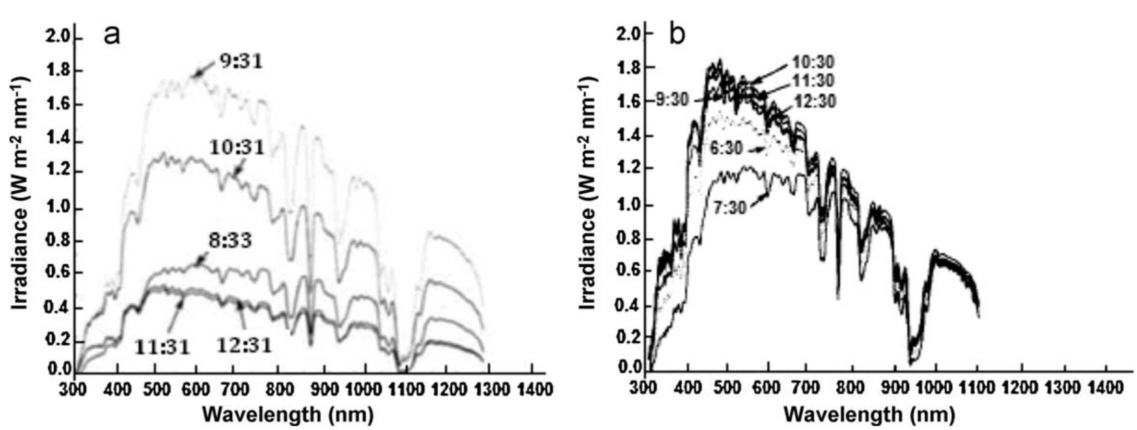


Fig. 21. (a) and (b) Global-normal spectral solar radiation on a cloudy day and a relatively clear day respectively (Riordan [31]).

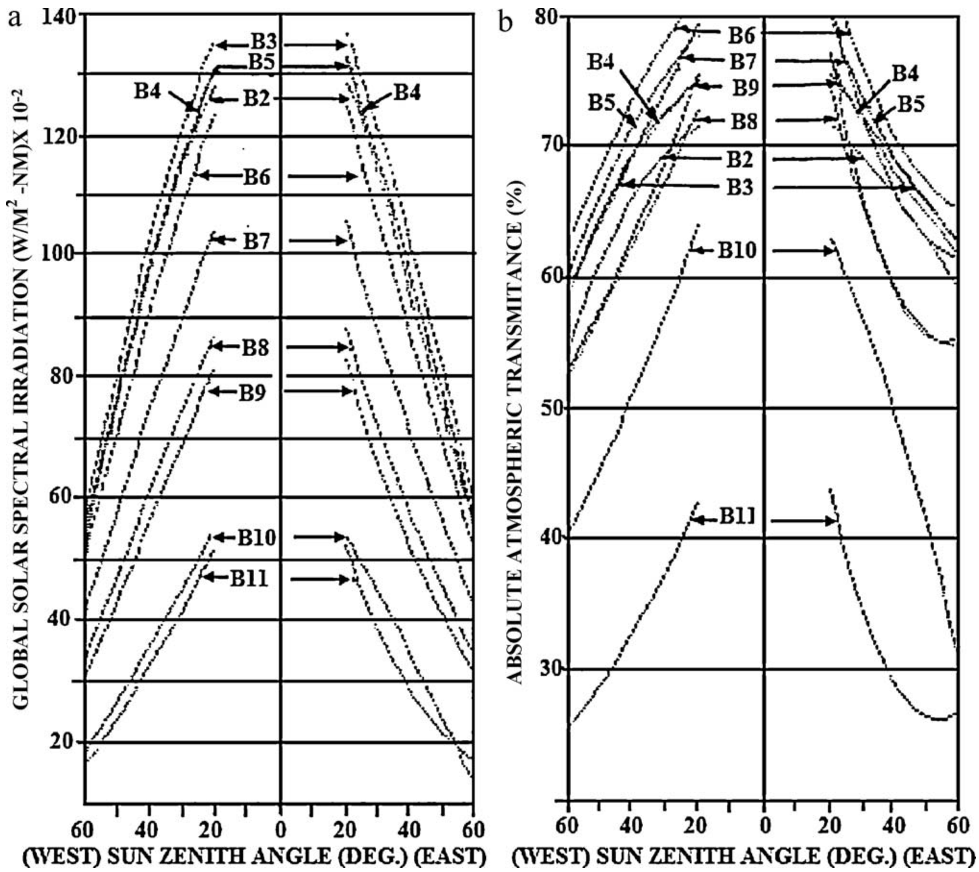


Fig. 22. (a) Best fit curves of global solar spectral irradiance w.r.t. sun angle for various bands. (b) Best fit curves of absolute atmospheric transmittance w.r.t. sun angle for various bands (Manjul and Verma [32]).

on the terrace of the Department building at a height of 40 m above sea level at 13:30 h on July 14, 1993 under clear sky conditions with optical masses ranging 1.05–4.50 in Burjassot, València, Spain. For the direct component, a radiance limiting tube with a field of view of 5° was coupled to the Teflon diffuser of the spectroradiometer receptor. For the diffuse component, a shade disk was used. Two scans were made for each measurement and the average value was saved into computer memory. This process required less than 90 s in total. The spectroradiometer was oriented manually on a tripod with the help of a three-axis joint and a system of alignment for the measurements in the direction normal to solar rays. On the other hand, global and ultraviolet integrated irradiance, on a horizontal plane were continually recorded in the same location by means of a Kipp-Zonen CM-6 pyranometer and Eppley TUVR, respectively. Fig. 23 displays the spectral distribution of direct, diffuse and global irradiance on the normal and horizontal planes on 14 July 1993, optical air mass 1.2 that was obtained.

Adeyefa et al. [34] measured the direct, global and the diffuse solar spectra in the wavelength range 300–1100 nm, for two non-consecutive months between December 1991 and February 1992, during Harmattan weather conditions with the LICOR LI-1800 spectroradiometer on the roof of the physics block at the Obafemi Awolowo University (O.A.U.), which is about 20 m high at Ile-Ife (7°30′N, 4°31′E, 370 m above sea level) which is situated in the south-western part of Nigeria. For the direct normal measurements, a screening tube with a 5° field of view was constructed to meet the recommendations of the WMO. The silicon photodiode detector of the spectroradiometer used has a temperature dependence which is a function of wavelength. During the measurements, the temperature of the detector was monitored using a thermistor attached to its housing. They observed there were severe reductions in the direct solar irradiance at Ile-Ife during this period due to the strong attenuating effects of the Harmattan dust as can be seen in Fig. 24.

On the other hand, a significant increase in the diffuse irradiance was observed which, in all the cases examined during the period, exceeded the direct irradiance.

Adeyefa and Holmgren [35] measured the ground-level spectral distribution of the direct, diffuse and global solar irradiance between 300 and 1100 nm at Akure (7.15°N, 5.5°E), Nigeria, in December 1991 before and during Harmattan dust spell employing a spectroradiometer (LICOR LI-1800). The LI-COR model LI-1800 spectroradiometer used for this study was a completely self contained, battery-operated and microprocessor-controlled spectroradiometer for rapid acquisition of spectral irradiance data. The heart of the LI-1800 system is its internal microprocessor which

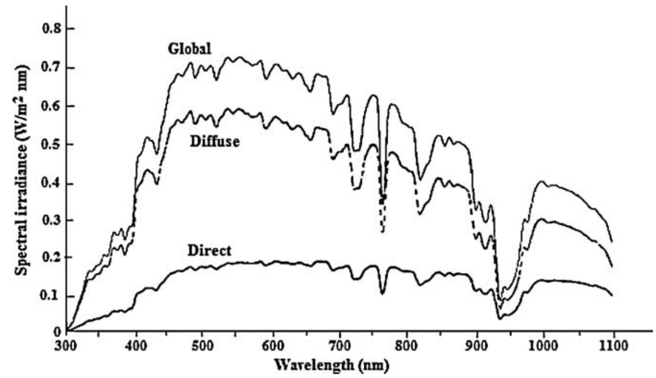


Fig. 23. Spectral distribution of direct, diffuse and global irradiance on the normal and horizontal planes on 14 July 1993, optical air mass 1.2 (Martinez et al. [33]).

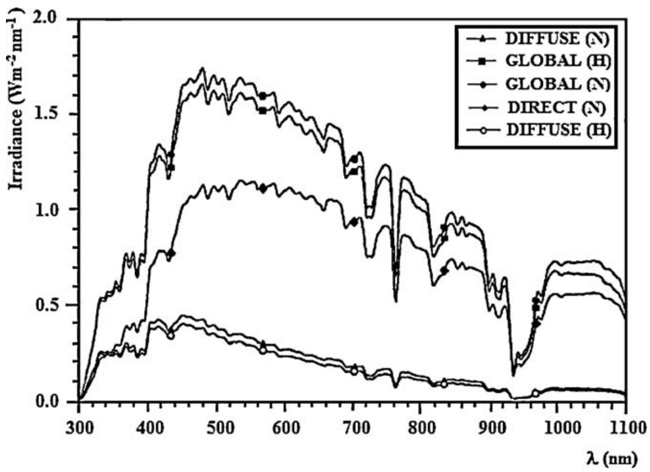


Fig. 24. Typical cases of direct normal, global horizontal and diffuse horizontal spectra measured with the LI-COR LI-1800 spectroradiometer at Ile-Ife, Nigeria, on 18 December 1991 (Solar elevation = 50.2°) (Adeyefa et al. [34]).

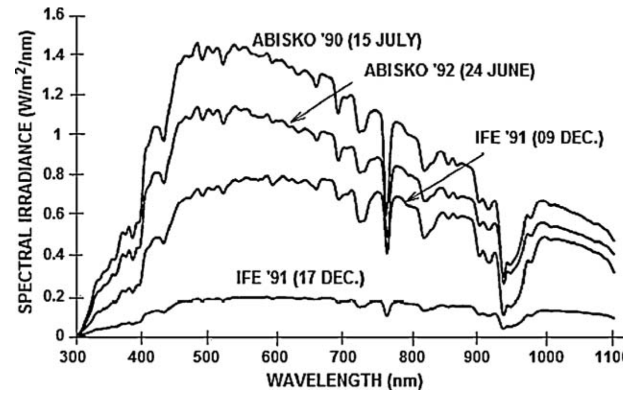


Fig. 26. Direct spectral irradiance under different turbidity conditions. Top curve, 15 July 1990, Abisko, Sweden; second, 24 June 1992, Abisko; third, 9 December 1991, Ile-Ife, Nigeria, before a harmattan spell; bottom, 17 December 1991, Ile-Ife, during the spell (Adeyefa et al. [36]).

handles all collection, storage, communication and manipulation of data files. The spectroradiometer has a spectral resolution of 6 nm with a wavelength accuracy of +2 nm. The results presented in this paper highlight the direct solar irradiance is reduced significantly as seen in Fig. 25. This reduction in the direct irradiance is significant particularly in the ultraviolet and visible spectral regions but is compensated, to some extent, by an increase in the diffuse component. The global irradiance is also reduced but is less sensitive to changing Harmattan conditions due to concurrent increases in the diffuse component.

Adeyefa et al. [36] compared the effects of atmospheric turbidity due to aerosols on the direct solar irradiance at the surface at a low latitude (Ile-Ife (7°30′N, 4°31′E), south-western Nigeria) and a high latitude station (Abisko (68°21′N, 18°49′E), northern Sweden) before and after the Pinatubo eruption between 15 July 1990 and 4 July 1994 at selected times during the summer half-years. At Ile-Ife data were collected between 5 December 1991 and 26 February 1992. The spectral solar radiation was collected with portable LICOR LI-1800 spectroradiometer (SRM) (wavelength range 300–1100 nm); resolution 6 nm and spectral accuracy ± 2 nm). The instrument was fitted with a screening tube in order to allow to measure the components of the solar radiation within a circular aperture of 2 × 2.5°.

The results of these measurements show that under intense harmattan conditions, the atmospheric turbidity at Ile-Ife is about 7

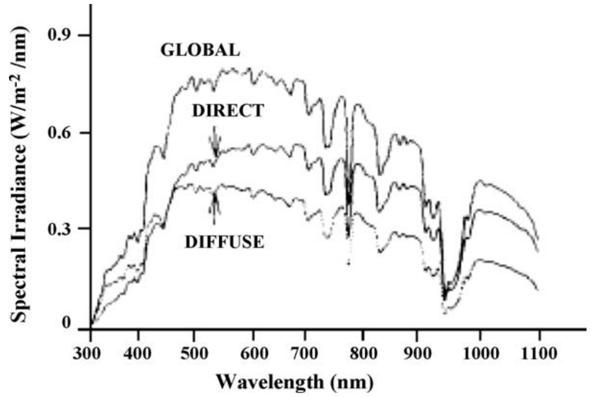


Fig. 25. An example of the quasi-simultaneous measurements of the direct-normal, global horizontal and diffuse-horizontal spectra with the spectroradiometer at Akure, Nigeria, on 13 December 1991 (m = 1.5; β = 0.5) (Adeyefa and Holmgren [35]).

times higher than that in the Arctic region, even with the significant effect of the Pinatubo volcanic eruption on the latter. Fig. 26 displays the effect of atmospheric turbidity on the spectral irradiances at the surface at the low-latitude station (Ile-Ife, Nigeria) the dramatic effects of the Saharan aerosols on the relation between the direct and diffuse components. During intense spells of harmattan the direct component became only a small fraction of the hemispheric diffuse radiation, with rather small changes over the spectral interval investigated. Before the Pinatubo The aerosol load at Abisko, above the Arctic Circle in northern Sweden, was below typical background levels considered for the northern hemisphere. After the eruption the aerosol loads increased dramatically, which had marked effects especially on the optical depths in the near infrared region.

Bernhard et al. [37] measured global spectral irradiance in the UV and visible range between December 24, 1995, and January 20, 1996 near Townsville, Australia, on the roof of the Physics Department of the James Cook University (JCU) of North Queensland (19.33°S, 146.76°E, 30 m above sea level (asl)) using the mobiles pectroradiometer of the Fraunhofer Institute for Atmospheric Environmental Research (IFU), Germany. At the beginning of the campaign, the solar elevation at noon was 86° and at the end, 89°. Most days were partly cloudy, but January 11 was nearly a clear sky day. Between January 5 and 8, heavy storms and rainfall occurred.

The mobile IFU spectroradiometer consists of a horizontal cosine-response diffuser coupled by quartz fiber optics to a double monochromator DTM 300 from Bentham instruments (focal length, 300 mm; focal ratio; j/4.1). For the wavelength range 285–500 nm, holographic gratings with 2400 lines mm^{-1} are used and radiation leaving the monochromator is chopped, detected with a bialkali-photomultiplie (9205QB, EMI) and amplified using lock-in technique. For wavelengths above 500 nm ruled gratings with 600 lines mm^{-1} are applied, the nominal bandwidth is 2 nm FWHM (measured 2.3 nm FWHM), and the radiation is detected with a Si-diode. Below 410 nm, measurements were taken in 0.25 nm increments and above 410 nm, in 1 nm steps. During the campaign, the whole system was maintained at 33 ± 0.5 °C and was fully controlled by a PC.

Approximately every 13 min, a spectrum of global spectral irradiance was measured between 285 and 1100 nm (650 nm after January 4). Fig. 27 shows a spectrum that measured at noon on January 11, 1996, a day with nearly cloudless sky; the global spectral irradiance in the UVB (280–315 nm) and UVA (315–400 nm) is plotted on a linear and logarithmic scale. The solar zenith angle (SZA) during the scan was approximately 3°.

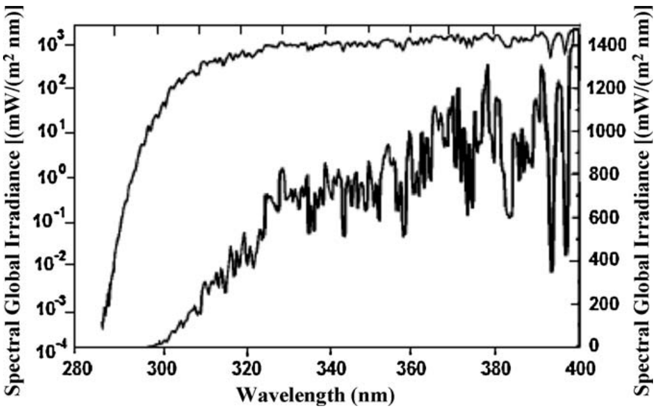


Fig. 27. Spectral global irradiance, January 11, 1996, 3° solar zenith angle (SZA) on a linear (right axis) and logarithmic (left axis) scale (Bernhard et al. [37]).

The spectra measured on January 11 were compared with results from the radiative transfer model UVSPEC, type pseudo-spherical, developed by A. Kylling. Both measured and modeled spectra were averaged over 10 nm wavelength bands, and the ratios were plotted as a function of time. Fig. 28 showed the diurnal variation of the ratios of measured and modeled global irradiance.

Bruce [38] used Analytical Spectral Devices Full Range (ASDFR) spectroradiometer conjunction with a simple, custom-designed telescope to make spectrally continuous measurements of solar spectral transmittance and directly transmitted solar spectral irradiance in the wavelength range from 350 to 2500 nm. The ASDFR consists of three separate spectrometers: a silicon photodiode array in the visible near infrared (VNIR, 350–1000 nm) and two scanning spectrometers in the shortwave infrared (SWIR, 1000–2500 nm). The two SWIR spectrometers designated SWIR1 for the 1000–1770 nm region and SWIR2 for the 1770–2500 nm region are single element, thermoelectrically cooled InGaAs detectors. The SWIR1 and SWIR2 gratings were attached to a motor that scans back and forth every 0.1 s. The position of the grating shaft, and thus the wavelength, was determined with an optical encoder. Instrumental dark current was measured and subtracted out from each spectrum prior to its recording in the SWIR1 and SWIR2. In the VNIR, the dark current was measured at the beginning of the measurement cycle, and masked detectors in the array thereafter track dark current fluctuations. The spectral sampling was approximately 1.4 nm in the VNIR and 2.0 nm in the SWIR.

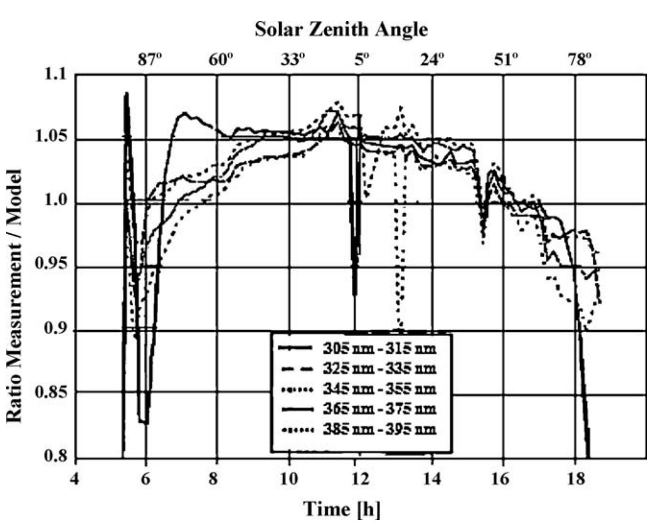


Fig. 28. Diurnal variation of ratios of measured and modeled global irradiance for January 11 (Bernhard et al. [37]).

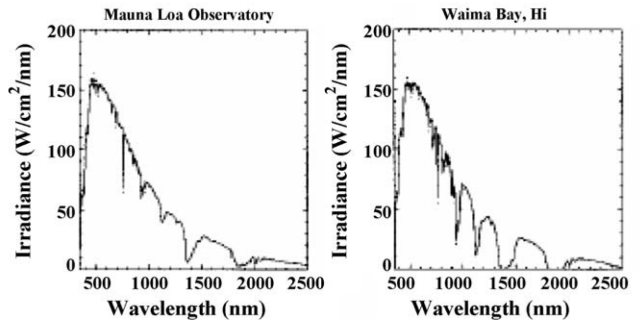


Fig. 29. (a) ASD-FR measured (solid curve) and the MODTRAN-modeled (dotted curve) direct solar irradiance for a measurement taken at MLO. (b) Same as (a) but for Waima Bay, Hawaii, with a higher water-vapor amount (Bruce [38]).

The telescope was designed for use with commercially available solar trackers to measure the direct normal solar spectral irradiance only that of the solar disk, approximately 0.5°. The telescope contains front and rear apertures and does not contain any optical elements. The apertures were removable and can be replaced easily with apertures of various sizes to increase or decrease the field of view (FOV). Attached to the rear of the telescope is a 0.05 m. Spectral on integrating sphere. On the top of the telescope a pinhole and target allow for precise alignment to the sun.

The ASDFR spectroradiometer outputs a spectrum that had been linearly interpolated to every nanometer, while sampling approximately only every 1.4 nm in the VNIR and 2.0 nm in the SWIR1 and SWIR2, so to assess the errors that might be produced by this interpolation they ran a simulation with MODTRAN. As an additional test of the suitability of the ASD-FR as a solar radiometer, they made a side-by-side comparison with the Reagan ten-channel solar radiometer. Fig. 29a and b displays MODTRAN4.0 model compared with two examples measurements were selected at random from the experiment undertaken in Hawaii in April 2000. One spectrum was selected from the measurements taken at MLO, and a second spectrum was selected from measurements taken on the west coast of Hawaii at sea level and thus containing a much higher column water-vapor amount.

Pérez-López et al. [39] used a spectroradiometer MONOLIGHT^{TM} model6602 whose measurement range is 250–2500 nm to study the effect of solar spectral variations that is extending the spectral range far away from the wavelengths where PV semiconductors are active in PV conversion. The four PV materials that considered in this work were (m-Si, a-Si, CIGS, CdTe). All measurements were taken on the roof of the building of the Renewable Energy Department of CIEMAT in Madrid (40.45°N, 3.73°W, 620 m above sea level). Solar spectra were measured only in selected clear days (no visible clouds), covering the four seasons of the year considering a horizontal receiver plane.

The resolution used during measurements was 1 nm and the scan time for the whole range of wavelengths ranges between 100 and 300 s (typically 120 s), depending on the intensity of the sunlight to be measured. The optical receptor of the spectroradiometer consists in an integrating sphere (6 in. diameter) having a hemispherical quartz dome (3.5 in. diameter). The input port of sunlight to the integrating sphere is a circular hole having a diameter of 2.2 in. located under the quartz dome. The monochromator system was made of two holographic gratings that were mounted in a moving platform that is rotating at a speed of 1 turn per second. The detectors, located at the exit slit of the monochromator, were Si (for 250–1095 nm wavelength range) and InGaAs (for the 1095–2500 nm wavelength range) photodiodes. Both detectors are thermoelectrically cooled to minimize temperature effects. The parameter that used to study the influence of the solar spectral irradiance in PV conversion was the Spectral Factor (SF) or Mismatch

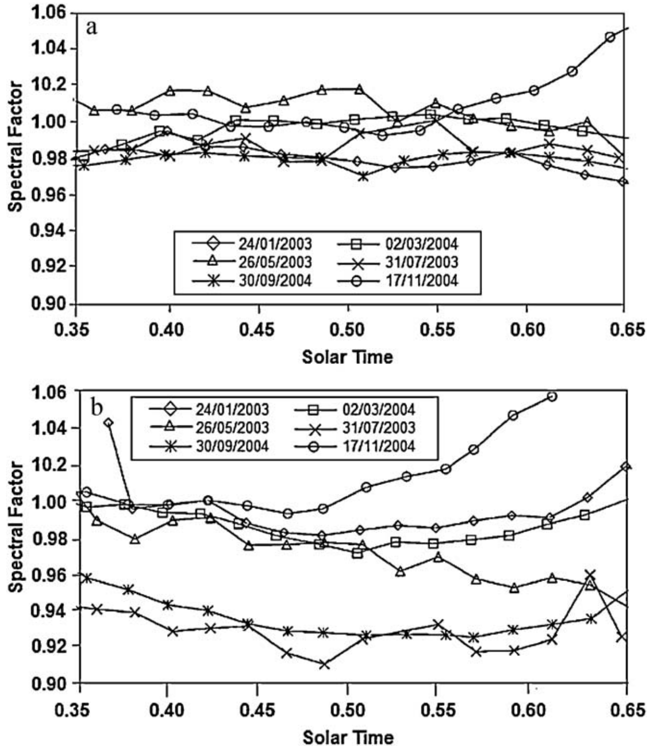


Fig. 30. (a) and (b) SFs for m-Si in and a-Si in different clear days respectively (Pérez-López [39]).

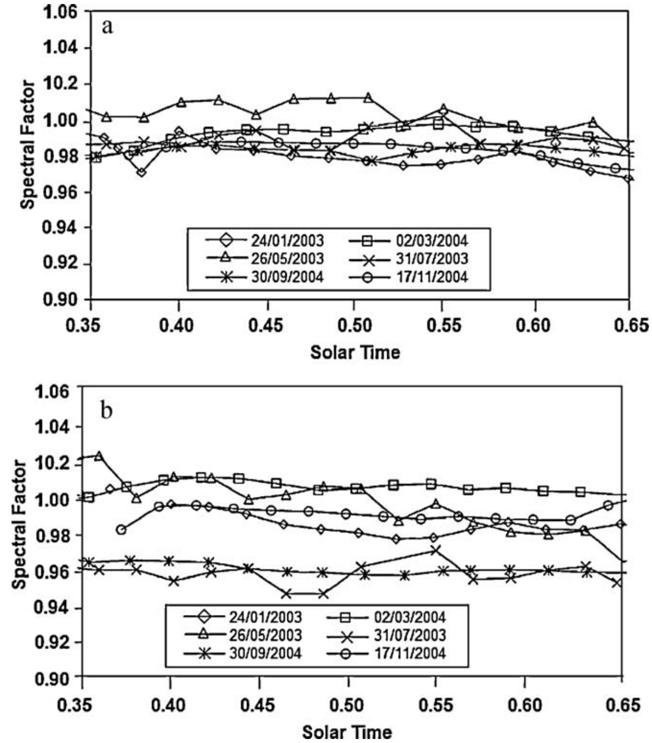


Fig. 31. (a) and (b) SFs for CIGS and CdTe in different clear days respectively (Pérez-López [39]).

Factor (MMF) which that can be defined as:

$$SF = \frac{\int E_{STD}(\lambda)SRr(c)d\lambda / E_{STD}(\lambda)d\lambda}{E_{STD}(\lambda)SRr(\lambda)d\lambda / \int E_{STD}(\lambda)d\lambda}$$

Figs. 30 and 31 show the daily evolution of the SFs calculated from solar spectra measured in different clear days (winter, spring, summer, and autumn) for the four PV materials considered in this work.

The results showed the PV conversion efficiency of semiconductors has to be a seasonal dependent issue because of natural solar spectrum variations: some materials were much more favored for operation in summer time (a-Si, CdTe) than in winter time (m-Si, CIGS). PV materials having narrow spectral responses (a-Si, CdTe) were much more sensitive to spectral effects than other PV materials with wide spectral responses (m-Si, CIGS).

Krezhova et al. [40] registered the spectral distribution and integral changes in the solar radiation reaching the earth's surface as well as images of the sun's disk from an observation post on the line of totality situated on the Black Sea coast using videospectrometric during the total solar eclipse on 11 August 1999 in the territory of Bulgaria. The videospectrometric included a CCD television camera with high sensitivity (optical resolution 400 lines mm^{-1}, spatial resolution of 500 × 582 elements), a photographic camera PRAKTICA, a high-resolution multichannel spectrometric system "Spectrum 256", a photometer J16 Tektronix, a computer system for experiment control and data recording, a diffuse white screen, and auxiliary technical means. The spectrometer operated in the visible and near infrared ranges (480–810 nm) in 128 spectral channels at a spectral resolution (halfwidth) of 2.6 nm. The time of each spectrum acquisition was 25 ms and the scanning speed was 40 spectra per second.

The partial eclipse started at 12^h46^m LT and ended at 15^h33^m LT. The duration of the total eclipse was 146 s. The measurements were carried out in intervals of 1 min between the 1st and 2nd (from 12^h44^m till 14^h05^m) and 3rd and 4th contacts of the eclipse (from 14^h17^m till 15^h30^m). 86 averaged spectra of the solar radiation reaching earth's surface have been obtained. A part of them (as can be seen in Fig. 32) recorded in interval of time 14^h17^m till 14^h52^m after the eclipse totality. The spectrometric data of the spectral solar distributions at time intervals equidistantly disposed before and after the eclipse totality were processed and compared by means of statistical method (Students't-criterion).

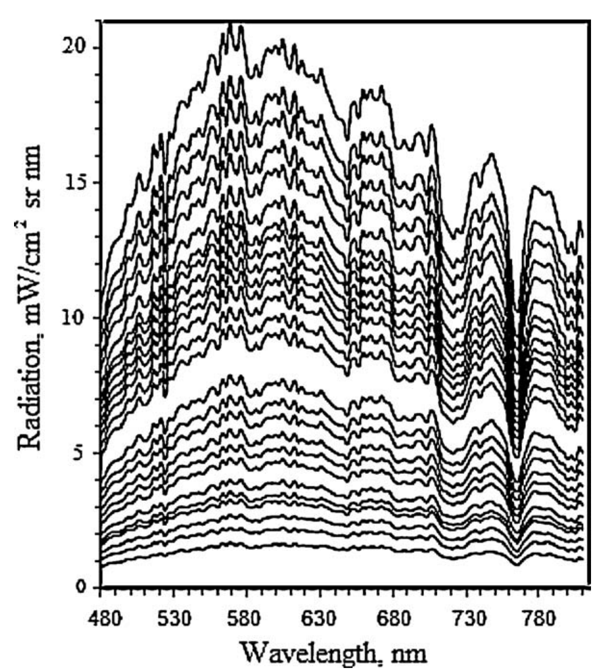


Fig. 32. The spectral distributions of the solar radiation in interval of time after the eclipse totality (Krezhova et al. [40]).

The results showed:

1. Regardless of the favourable atmospheric conditions during the measurements changes were registered in the solar radiance within the limits of 1–2% immediately before and after the eclipse totality.
2. The examination of the solar radiation dynamics revealed presence of fluctuations in the recorded spectral distributions before and after the eclipse totality expressed in a weak redistribution of the solar energy in the spectral range (480–810 nm) in the limits of 1–2%.
3. The applied statistical method (Students'*t*-criterion) proved statistically significant differences at a probability level of $p < 0.001$ between the spectral distribution of the solar radiation recorded at time intervals disposed equidistantly before and after the eclipse totality.

Krezhova et al. [41] measured the visible and near-infrared radiation ranges (350–1000 nm) during the total solar eclipse on March 29, 2006 at the Antalya region near the coastal town Manavgat (latitude 38°01′; longitude 32°31′) on the Mediterranean Sea coast, Turkey, using a general-purpose USB2000 fiber optic spectrometer (Ocean Optics, 2005). The spectrometer was operated in the visible and near-infrared ranges (350–1000 nm) at a spectral resolution (halfwidth) of 1.5 nm. It has a 25 mm entrance aperture and a 2048-element linear silicon CCD array. The measuring entrance lens is at the end of a flexible light guide. A total of 45 spectra were obtained between the 1st and 2nd contacts. A few of these, recorded in the time interval 12 h 36 min till 13 h 45 min, are presented in Fig. 33.

The results of those measurements showed the

1. The spectral characteristic with the highest values of spectral radiance was recorded at 12 h 36 min.
2. Overall decrease of the radiance with time, related with a decrease of irradiating energy as the sun's disk is increasingly occulted by the moon up to the 2nd contact.

Polo et al. [42] measured the direct-beam spectral solar irradiance during one year at solar platform of Almería (PSA) meteorological station (37.09°N, −2.36°E, 560 m above sea level), located in the desert of Tabernas, in the south-east of Spain, with commercial SP302D, double monochromator spectroradiometer from instrument systems company, in the spectral range of 280–900 nm with a wavelength step of 2 nm, to estimate Angstrom parameters (turbidity and wavelength exponent) and total ozone column. The direct-beam probe of the spectroradiometer was mounted on a two-axis solar tracking system and it automatically takes a measurement every 20 min from sunrise to sunset. The spectroradiometric accuracy was of 5% within this spectral range and the absolute wavelength accuracy is ±0.03 nm. The spectroradiometer SP320 D was calibrated at instrument systems laboratory during the spring 2005.

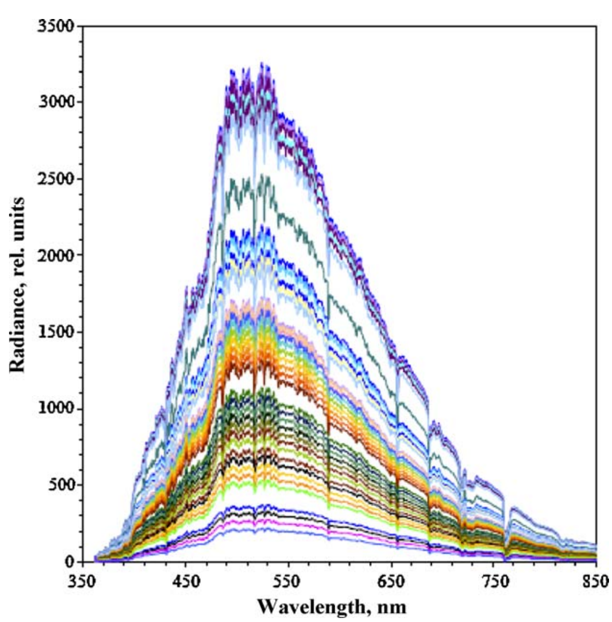


Fig. 33. The spectral distributions of the solar radiation in interval of time between the 1st and 2nd contacts of the total solar eclipse on March 29, 2006 (Krezhova et al. [41]).

3.2. Ultraviolet

3.2.1. Overview

The term ultraviolet, often abbreviated as UV (Coulson [43]) is defined as the portion of the electromagnetic spectrum between X-rays and visible light, which is between wavelengths of 40 and 400 nm (energy comprised between 30 and 3 eV). The UV spectrum can be divided into broad bands: vacuum UV (40–190 nm), far or extreme UV (190–220 nm), UVC (220–290 nm), UVB (290–320 nm), and UVA (320–400 nm). Only the last three bands of solar radiation (UVC, UVB and UVA) reach the earth's atmosphere (Pinedo et al. [4]) and due to natural fluctuations in earth's atmosphere throughout the annual cycle and unnatural changes brought about by the introduction of air pollutants (Kimlin [44]) only the last two (UVB and UVA) reach the earth's surface (Pinedo et al. [4]). The ultraviolet solar spectrum is very rich in detail, due to numerous emission and absorption lines of the different elements in the solar chromosphere and corona (Coulson [43]).

3.2.2. Detection systems

Measurements of solar ultraviolet irradiance (UVI) started in the first decades of the 20th century with chemical detectors, where the changing of the color of a solution was an indicator of UVB irradiance. Physical measurements of UVI use photoelectric methods to give quantitative information about the intensity and spectral distribution of UVI. The first extensive data sets originate from the 1960s, from Davos (Switzerland), but it was not until the 1990s that more of such high quality spectral measurements were made at further locations world-wide. Since the 1970s a greater number of UV measurements have been made with a different type of detector, sensitive to a broad wavelength range in the UVB (and to a lesser extent in the UVA), the so-called broadband erythermal detectors. They have been used in many parts of the world for monitoring over periods of several years, but systematic, long-term observations are rare and again were mainly established in the 1990s in response to stratospheric ozone depletion (Helbling [45]).

The characteristics of the measurement and detection system used and its calibration are important in determining the measurement accuracy. These, combined with the geometrical and physical factors affecting the quantity and quality of solar radiation, make comparisons of UVI measurements made with different systems extremely difficult. Desirable features in a measurement and detecting system include stability, adequate sensitivity, low background response and known and reproducible wavelength and angular response characteristics.

Four main types of system are used to obtain information relating to solar UVI levels:

1. Spectroradiometric monitoring equipment (which measures solar UVI at each wavelength interval over a wavelength range generally from ≈290 to 400 nm).

2. Brewer spectrophotometers (ground-based instruments providing information from optical radiation measurement of total ozone and UVI irradiance).
3. Broad-band measurement equipment (providing instantaneous measurement over selected wavelength ranges of biologically weighted irradiance or filtered flux).
4. Personal UVI dosimeters (generally small broad-band or chemical detectors to provide the integrated weighted UVI dose at various body locations).

There are three main problems related to the collation and comparison of data from these measurements:

1. Lack of standardization of instrumentation where different instruments with different characteristics and precision have been used, making any correlation of the results from different organizations difficult.
2. Inconsistencies in cross-calibration of measurement equipment used by different organizations at various sites, where a variety of calibration sources with different characteristics have been used.
3. Lack of continuity of measurement and incompatibility of data acquisition systems and data formats.

3.2.2.1. Spectroradiometers. A spectroradiometer measures irradiance within a narrow bandwidth, centered at a wavelength, which is selected by the operator, and is continuously variable. The basic components to illustrate the principles of operation are:

1. input optics;
2. monochromator;
3. detector.

Optical radiation is collected by the input optics, which should possess a 2π field of view and a cosine weighted angular response. Two types of input optics achieve these requirements. A transmission diffuser at the entrance slit of the spectroradiometer can produce an approximate cosine response. Alternatively, this can be achieved with an integrating sphere with a small entrance aperture and an internal diffuse coating, such as MgO or $BaSO_4$, with a high UVI reflectance. A second aperture in the integrating sphere provides input for the optical radiation via an entrance slit to a monochromator.

The entrance slit of the monochromator is at the focal point of a collimating mirror and optical radiation is reflected from the mirror as a parallel beam incident on a ruled diffraction grating, producing on angle. A second mirror collects optical radiation from the grating at a particular angle (hence wavelength) and focuses it onto the exit slit of monochromator. High performance spectroradiometer, used for determining low irradiances of UVI, require low stray radiation levels and use a double grating monochromator.

An appropriate detector such as a photomultiplier tube or occasionally a photodiode, is mounted at the detector is integrated for a pre-selected time and then is transferred to a microcomputer for storage and display. The wavelength drive and output integration are synchronized to provide a spectral scan of irradiance in equal wavelength intervals throughout a given optical spectrum.

The UVI spectral measuring capabilities of Brewer spectroradiometers (used for ozone column measurements) can be exploited to measure the solar spectral irradiance in the wavelength region 290–325 nm (i.e. principally UVB), although these instruments do have limitations in precision below 310 nm (Driscoll [46]).

3.2.2.2. Broadband instruments. Spectroradiometers are capable of high precision in the measurement of spectral irradiance, but they are expensive. Less precise estimates of $E(\lambda)$ or E_{eff} are achievable with less expensive broad-band instruments, which integrate spectral irradiance over a range of wavelengths. Physical phenomena used in two measurement methods are (a) thermal, where energy absorption results in a measurable temperature change in a detector; and (b) photoelectric, which involves a conversion of UVI into an electrical signal.

3.2.2.2.1. Thermal detectors. Thermal detectors have a uniform response within their region of operation and are particularly useful for the absolute determination of irradiance and as such are often used as calibration instruments.

There are two types of thermal detector for operation with UVI

1. A thermopile, which depends on the Seebeck effect, whereby a voltage is generated when heat is applied to the junction of two dissimilar metals. A fused silica window is used in a thermopile for UVI operation and the instrument will operate with a near flat response over the wavelength range 180–3400 nm. Heat losses in a thermopile can result in nonlinearity in response, particularly at high irradiances (e.g. greater than $\approx 300\,\mathrm{W\,m^{-2}}$). Thermopiles should not be used for irradiances greater than $2000\,\mathrm{W\,m^{-2}}$.
2. A pyroelectric detector, which depends on a voltage generated by temperature change via a change in electrical polarization in a crystal, such as lithium tantalite. A pyroelectric detector has a faster response than a thermopile and a typical irradiance range of 10^{-4}–$10^{6}\,\mathrm{W\,m^{-2}}$.

3.2.2.2.2. Photoelectric detectors. There are a range of devices employing photoelectric detector for UVR measurement, some of these devices provide a measurement of $E(\lambda)$ and some with the addition of optical filters provide an assessment of E_{eff}. The photoelectric detectors used in such devices include:

1. photomultiplier tubes;
2. vacuum photodiodes;
3. silicon photodiodes;
4. GaAsP photodiodes.

Three commonly used devices which employ this technology for health hazard assessment and environmental monitoring in the UVR spectral region are the direct reading radiometer, the filtered UVR meter and the Robertson–Berger (R–B) meter.

3.2.2.3. Personal dosimeters. The biological effective UVR dose applied to the body over a time interval $T(s)$ is defined as

$$D = \sum_{t}\sum_{\lambda} E(\lambda, t) A(\lambda) d\lambda dt$$

where $E(\lambda,t)$ is the spectral irradiance and $A(\lambda)$ is the appropriate biological action spectrum.

3.2.2.3.1. Film dosimeter. Changes in the optical properties of photosensitive films to incident UVI can be used in UVI personal and environmental dosimetry. These dosimeters provide a simple means of integrating UVI exposure continuously and because they are cheap and compact can be used for environmental measurements at many locations inaccessible to bulky instrumentation.

3.2.3. Measurements of spectral solar UV irradiance in the tropic

Wong and Parisi [47] measured the spectral irradiance of ambient UVA (320–400 nm) under a clear sky conditions at around 12:00 noon Eastern Standard Time (EST) in Brisbane, Australia in mid summer and in mid winter during the period between 1994 and 1995 with spectroradiometer.

Roy et al. [48] used installed spectroradiometer (SRM) at Yallambie (37.8°S) and Davis (69.0°S) in Antarctica and portable SRM at other locations in Australia and overseas to measure spectral solar ultraviolet radiation in the range 290–400 nm. The pc-controlled SRM incorporates Spex 1680Bdouble grating monochromator, and the detector is an EMI 9653QA end-on photomultiplier tube cooled to −10 °C which is connected with a Keithley 616 digital electrometer to Measure the current.

Mikhalev et al. [49] measured the solar ultraviolet radiation on the ground during the solar eclipse that was observed on March 9, 1997, in the northern part of the eastern hemisphere in the area with the coordinates 49°N and 87°E on the border between Russia and the People's Republic of China with an original automatic spectrophotometer in the wavelength range 296–326 nm at intervals of 5–10 min, and at some instant of time in the range 306–346 nm. The spectrophotometer was made on the basis of universal spectral computational complex KSVU-12. Input–output multifunction board LA-2 and IBM PC 286 (386) were used as a spectral information collection system. The spectral resolution was 0.25 nm, and the scanning rate was 8 nm min^{-1}. The results of these measurements showed the short-duration changes in spectral distribution of the ground-level ultraviolet radiation were recorded during time intervals near the maximum phase and at the end of the solar eclipse. Changes in spectral distribution of the UV radiation near the onset time of the eclipse maximum phase are interpreted as an increase in the share of the multiply scattered radiation during this time interval.

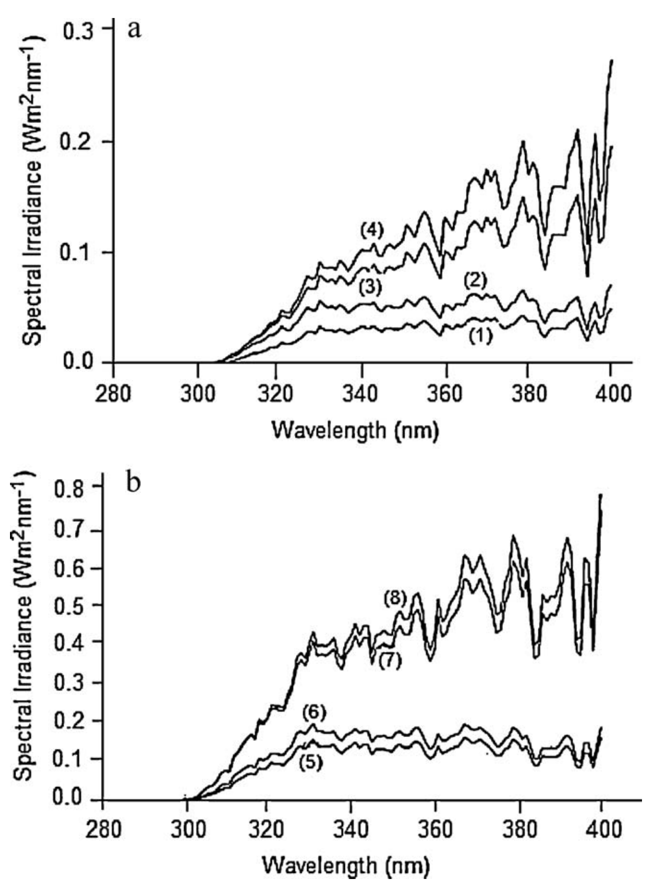


Fig. 34. Eight UV spectra for 3rd September for early morning and near noon. The spectra are: (a) (1) sun-normal and diffuse UV at 08:52 EST, (2) horizontal and diffuse UV at 08:57 EST, (3) horizontal and total UV at 08:55 EST, (4) sun-normal and total UV at 08:49 EST; (b) (5) sun-normal and diffuse UV at 10:54 EST, (6) horizontal and diffuse UV at 11:00 EST, (7) horizontal and total UV at 10:57 EST and (8) sun-normal and total UV at 10:50 EST (Parisi and Kimlin [50]).

Parisi and Kimlin [50] measured the solar UV spectrum in the range wavelength from 280 to 400 nm on mostly cloud-free days in an open unshaded field at a sub-tropical Southern Hemisphere latitude for the solar zenith angle range 35–64°, in late winter and early spring on 10 August and 3 September, 1998 in Toowoomba (27.5°S), Australia, with spectroradiometer based on a double holographic grating (1200 lines mm^{-1}) monochromator (model DH10, Jobin-Yvon France) connected to a R212 photomultiplier tube (Hamamatsu, Japan) temperature stabilized to 15 ± 0.5° C and fitted with 15 cm diameter integrating sphere (model OL IS-640, Optronics Laboratories, Orlando, FL, USA) that can be manually orientated was employed. Eight UV spectra had been taken for 3 September for early morning and near noon (Fig. 34). The spectra are: (a) (1) sun-normal and diffuse UV at 08:52 EST, (2) Horizontal and diffuse UV at 08:57 EST, (3) horizontal and total UV at 08:55 EST, (4) sun-normal and total UV at 08:49 EST; (b) (5) sun-normal and diffuse UV at 10:54 EST, (6) horizontal and diffuse UV at 11:00 EST, (7) Horizontal and total UV at 10:57 EST and (8) sun-normal and total UV at 10:50 EST.

Pinedo et al. [4] measured the global ultraviolet spectral irradiance in the range 290–400 nm at Zacatecas, near the Tropic of Cancer, located at 2500 m above sea level, latitude of 22°N and longitude of 102°W, Mexico on May 3rd between 10:00 and 14:00 h, with corresponding solar zenith angles between 7° and 50°, and November 6th, between 12:00 and 14:00 h, local time corresponding to the peak hours in solar intensity, 2005 by using Benthan spectroradiometer with 0.5 nm step in wavelength or less. Fig. 35a and b presents six UV spectra measured on May 3rd 2005 between 10:00 and 14:00 h, with corresponding solar zenith angles between 7° and 50°, eight spectra measured on November 6th between 12:00 and 14:00 h, local time, corresponding to the peak hours in solar intensity respectively.

The results of these measurements showed relatively high levels of ultraviolet irradiance (UV), during peak daylight hours, which may be characteristic of areas close to the Tropic of Cancer.

3.2.4. Measurements of spectral solar UV irradiance outside the tropic

Feister and Gericke [51] used three instruments; Brewer spectroradiometer of the type MKII#30 (single monochromator), MKII#18 (double monochromator and a Bentham spectroradiometer DM 150 (double monochromator with optics fiber and diffuser) at the Potsdam Observatory (52°22′N, 13°5′E, 109 m asl), Germany, during the years 1995 and 1996, to cover different spectral ranges in the UVA and UVB regions with step widths of 0.5 nm and full

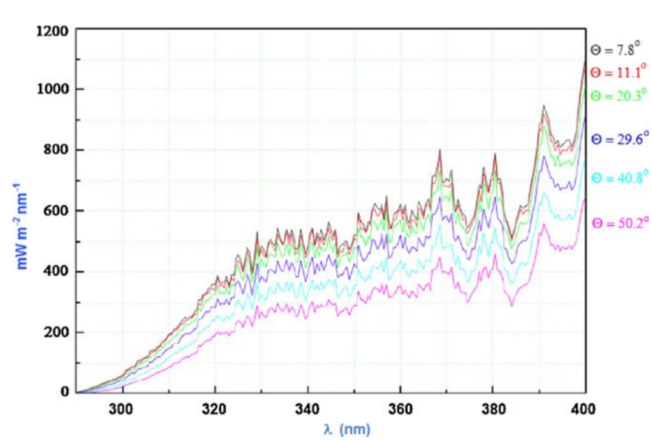


Fig. 35. (a) UV global irradiance spectra measured under clear sky condition on November 6th 2005. (b) As in Fig. 13a but on May 3rd 2005 in Zacatecas, Mexico. Solar zenith angles between 7° and 50°; measured between 10:00 and 14:00 h (Pinedo et al. [4]).

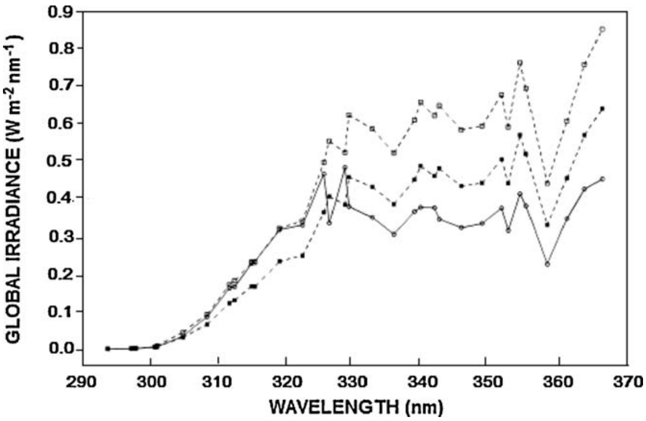


Fig. 36. Short-scan UV spectrum measured with Brewer spectroradiometer #118 at Potsdam on June 16, 1997 at 11:31 UTC (solid curve) and clear-sky spectra modeled for two different aerosol optical thicknesses τ_{550} = 0.01 and 1.0, respectively (dashed curves) (Feister and Gericke [51]).

bandwidths at half maximum FBHM between 0.5 and 0.6 nm. The measurements were carried out from sunrise to sunset with at least two spectral scans of global irradiance per hour taken by the Brewer instruments – in addition to spectral scans on direct sun, as well as measurements of total ozone taken by the same instruments – and 6 measurements per hour taken by the Bentham instrument. As an example, a spectrum of global UV irradiance June 16, 1997 distorted by a moving cloud is shown in Fig. 36.

Gröbner et al. [52] used the transportable reference spectroradiometer QASUME (Quality Assurance of Spectral Ultraviolet Measurements in Europe) to study the Quality of spectral solar UV instruments at 25 independent European laboratories to be as a European irradiance reference. A summary of the sites and the site instruments can be found in Table 2. The transportable QASUME reference spectroradiometer System consists of a commercially available Bentham DM-150 double monochromator with an effective focal length of 300 mm and a 2400 lines mm^{-1} grating. The wavelength range is 250–500 nm and the entrance and exit slit width were chosen to yield a near triangular slit function with a full width at half maximum resolution of about 0.8 nm. The solar irradiance was sampled through a specially designed entrance optic (CMS-Schreder Model UV-J1002). An end-window type bialkali PMT (electron tubes 9250QB) was used as a detector. The whole spectroradiometer system including the data acquisition electronics was contained in a temperature controlled box which was stabilized at a predetermined temperature with a precision of 0.5 K.

The measurement schedule was to measure global spectral solar irradiance in the range 290 nm to 450 nm or the maximum common wavelength at intervals of 0.5 nm. The measurement at each wavelength setting was time-synchronized to minimize variability induced by changes in solar zenith angle. The measurements covered all solar zenith angle SZA below 85° and were spaced at half-hour intervals. The spectra measured by each instrument were converted to 1 nm resolution using version 3.075 of the SHICRivm software package. Out of the 27 instruments 13 showed deviations relative to the QASUME reference spectroradiometer of less than 4% in the UVB (15 instruments in the UVA) for solar zenith angles below 75°. The results have shown the unique possibilities offered by this transportable reference spectroradiometer for providing onsite quality assurance of solar ultraviolet irradiance measurements.

Ren et al. [53] measured both broadband and spectral UV radiation from 24 June 1996 to 10 December1997 and from 28 November to 3 December 1997 respectively at Lhasa (29°40′N, 91°08′E, 3648 m above sea level) on the Tibetan Plateau, China, with a moderate bandwidth filter instrument (NILUV) and Fixed Imaging Compact Spectrometer (FICS) respectively. The broadband solar ultraviolet instrument has three channels centred on 305, 320 and 340 nm, respectively. It consists basically of a Teflon diffuser, filters and photo-diodes as detectors. It measures the global irradiance in these three channels with a full band-width at half maximum (FWHM) of 09 nm. A spectrograph, an imaging detector and three fiber optic inputs basically were conducted with FICS. A Teflon diffuser was mounted in front of one of these fiber optic inputs to enable the measurement of spectral global irradiance. Comparisons

Table 2
Site instrument characteristics. The instruments using the UV-J1002 diffuser do not correct their measurements for angular response errors since the angular response of the UV-J1002 diffusers is very close to the desired cosine response (Gröbner [52]).

Site instrument ID	Spectro radiometer type	Model	Monochromator	Temperature stabilized	Diffuser model	Data casine corrcted
Austria innsbruck ATI	Bentham	DTM300	Double	Y	UV-JI002	N
Germany, Hannover DEH	Bentham	DTM300	Double	Y	UV-JI002	N
UK, Manchester GBM	Bentham	DTM300	Double	Y	UV-JI002	N
Belgium, Brussels BRU	Bentham	DTM300	Double	Y	UV-JI002	N
Austria, Vienna ATW	Bentham	DMI50	Double	Y	UV-JI002	N
Norway, Troundheim NTN	Bentham	DMI50	Double	Y	UV-JI002	N
UK, Reading UKR	Bentham	DMI50	Double	Y	UV-JI002	N
Norway, Oslo NRP	Bentham	DMI50	Double	Y	Custom	N
Germany, Neuherberg BFS	Bentham	DMI50	Double	Y	Flat teflon	N
France, Briancon FRB	Bentham	DMI50	Double	Y	Flat teflon	N
EU.JRC, Ispra ISQ	Brewer#163	MKIII	Double	N	Custom	N
Finland, Jokioinen FIJ	Brewer#107	MKIII	Double	N-corrected	Flat teflon	Y
Greece, Thessaloniki GRT	Brewer#86	MKIII	Double	N	Flat teflon	Y
Belgium, Brussels RMI	Brewer#178	MKIII	Double	N	Flat teflon	N
Italy, Lampedusa LMP	Brewer#123	MKIII	Double	N	Flat teflon	N
Germany, Lindenberg DWD	Brewer#118	MKIII	Double	N	Flat teflon	N
Spain, EL Arenosillo AIS	Brewer#150	MKIII	Double	N	Flat teflon	N
Sweden. Norrkoping SEN	Brewer#128	MKIII	Double	N	Flat teflon	N
Belgium, Brussels KMI	Brewer#16	MKII	Single	N	Flat teflon	N
Portugal, Lisbon IML	Brewer#47	MKII	Single	N	Flat teflon	N
Finland, Sodanky Iä	Brewer#37	MKII	Single	N	Flat teflon	Y
Italy, Rome ITR	Brewer#67	MKIV	Single	N	Flat teflon	N
Czech Republik, Hradec Kralove CZH	Brewer#98	MKIV	Single	N	Flat teflonn	N
Poland, Warsaw PGI	Brewer#64	MKIV	Single	N	Flat teflon	N
EU.JRC, Ispra ISP	Brewer#66	MKIV	Single	N	Flat teflon	Y
France, Lille FRL	Jabin Yvon	HD10	Double	Y	Flat teflon	Y
The Netherlands, RIVM, NLR	Dilor	XY50	Double	Y	Flat teflon	Y

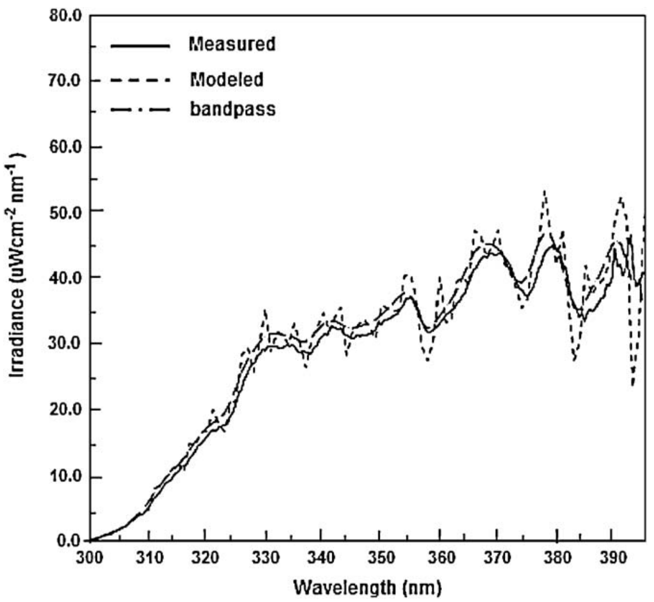


Fig. 37. Irradiance measured with FICS and calculated with the DOM model on 28th November 1997. The solid line shows the measured irradiance; the dotted line shows the originally modeled irradiance, while the dashed line shows the modeled spectrum after applying the bandpass function (Ren et al. [53]).

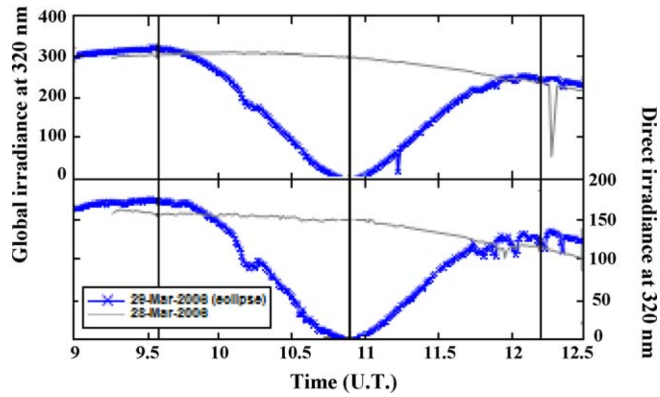


Fig. 38. Global (top) and direct (bottom) spectral irradiance at 320 nm measured with the Brewer spectroradiometer on the eclipse day (blue symbols) and on the previous day (grey lines) (Kazadzis et al. [54]). (For interpretation of the references to color in this figure legend, the reader is referred to the web version of the article.)

of both the broadband measurements and spectral measurements with the outputs of a discrete ordinate method (DOM) radiative transfer model had also been conducted.

The results from the comparisons of broadband measurements with model outputs showed that a 15, 11 and 10% agreement may be achieved around solar noon (with solar zenith angle smaller than 60°), respectively. The comparisons of the measured spectral irradiance with model calculations Fig. 37 indicate that large discrepancies may appear at wavelengths shorter than 209 nm and longer than 279 nm.

Kazadzis et al. [54] investigated the effect of the limb darkening on measurements of several radiation quantities (global irradiance (GI) which is the irradiance measured on a horizontal surface, the direct irradiance (DI) which represents the direct sun irradiance component and actinic flux (AF), which represents the radiation measured by a spherical surface at the island of Kastelorizo, Greece, during 28 and 29 (eclipse day) March 2006. Also total ozone column has been calculated from the DI measurements at the standard Brewer Ozone wavelengths (306.3, 310.1, 313.5, 316.8 and 320.1 nm) that were conducted during the campaign with the Brewer MK III. In addition, RTM System for Transfer of Atmospheric Radiation (STAR) calculations of the ET solar spectrum proposed by Köpke et al. (2001) were used in order to investigate temporal and spectral variability of UV irradiance during the solar eclipse of 29 March 2006.

The weather on 28 March was clear with cloudless skies and excellent visibility. On 29 March cirrus clouds started to form after the beginning of the eclipse. Occasionally, the cirrus clouds obscured the sun, especially after the time of the totality, affecting mainly the measurements of the DI. Various instruments deployed at Kastelorizo during this two-day campaign. A double monochromator spectroradiometer (Bentham DTM 300-UI), operating in the spectral range 290–400 nm in steps of 0.5 nm, has been used to measure simultaneously GI, AF and in addition DI. The full width at half maximum (FWHM) for the GI and AF measurements was 0.95 nm, while for the DI it was 0.55 nm. The scanning time for a full spectrum was about 3 min. A second double monochromator spectroradiometer (Brewer MK III-AUTH) has also been used to measure GI and DI in the wavelength region of 290–366 nm in steps of 0.5 nm and with spectral resolution of 0.55 nm (FWHM). For this study the operating software of the instrument was modified to allow the alternating measurement (every 30 s) of global and direct spectral irradiance at 6 wavelengths between 302 and 320 nm. Two diode arrays (PDA-UMAN) and a coupled charged device (CCD-AUTH) spectrometers (all single monochromators) were also used to record spectral measurements of GI, DI, AF and zenith radiance. Measurements of GI and DI during the eclipse and for the previous day are shown in Fig. 38.

The results

1. The decrease in total ozone is an artifact due to the increasing contribution of diffuse radiation against the decreasing direct irradiance (that is used for the total ozone column retrieval) caused by the eclipse.
2. Global irradiance, direct irradiance and actinic flux measurements showed that all quantities are spectrally affected by the limb darkening during the eclipse.
3. Calculations of the ET solar spectrum and the effective sun's temperature as derived from direct irradiance measurements at the surface, showed an artificial change in both quantities.
4. Calculations of the Extraterrestrial spectrum and the effective sun's temperatures, as measured from ground based direct irradiance measurements, showed an artificial change in the calculations of both quantities due to the fact that radiation coming from the visible part of the sun during the eclipse phases differs from the black body radiation described by the Planck's law.

4. Extraterresterial solar radiation measurements

Most of the energy produced in the fusion furnace of the sun is transmitted radially as electromagnetic radiation, popularly called sunshine or solar energy (Willian [55]). Considering the sun's temperature of 5760 K, the total power emitted by the sun is about 3.8×10^{30} W or 6.25×10^{11} W m^{-2}. Because of the large distance between the sun and the earth, the amount of solar radiation that reaches just outside the earth's atmosphere is quite low. It is only 1367W m^{-2}. This number is called the total solar irradiance (TSI) or the solar constant (Calisesi [6]). Solar constant is measured at the surface perpendicular to the sun's rays at the average sun–earth distance on the top of the atmosphere (Mora [17]). The intensity of solar radiation above the atmosphere varies approximately sinusoidally over the year with an amplitude of close to 3.3% of the solar constant and a maximum near the first of January (Webster [2]). This variation depends on the geometry of the globe, its rotation, and its elliptical, the eccentricity of the orbit, and the longitude

of the perihelion. Variation in the solar radiation is also caused by the difference in the emission intensity from the sun itself (Mora [17]).

Webb et al. [56] made Six flights onboard the NASA's Convair 990 research aircraft over the Pacific and western United States at an altitude of 11.58 km during August of 1967 to measure the solar spectral irradiance using a Leiss double prism monochromator and a GSFC modified Eppley Mark V radiometer. Measurements were made from special observation windows which had been cut into the fuselage at an angle of 65° from the horizontal. The ports used by the Leiss and filter radiometer were fitted with 2.5-cm thick plates of Dynasil 4000 quartz.

The Leiss monochromator is a double prism instrument designed to provide high dispersion with a minimum amount of stray light. The spectral range covered was from 0.3 μm to 1.6 μm, which contains about 90% of the sun's energy. The detector housing was mounted at the rear of the Leiss and contained two detectors—an EMI 9558 photomultiplier tube and a Kodak Ektron lead sulphide cell. The other instrument that was used was a photoelectric filter wheel radiometer which covered a spectral range from 0.3 μm to 1.1 μm using narrow band filters. Instrument calibrations were performed in flight using an NBS type quartz-iodine standard of spectral irradiance. The resulting spectral curves from the two instruments are shown in Fig. 39. Excellent agreement is noted between the two instruments through a wavelength range of 0.3–1.1 μm, even though they are optically and electronically dissimilar.

Woods et al. [57] used three solar EUV instruments from LASP; The EUV Solar Irradiance Experiment (ESIE) to measure the solar spectral irradiance from 30 to 110 nm with 0.1 nm resolution, XUV photodiodes to cover the spectral irradiance from 5 to 100 nm with about 15 nm and XUV imager to image the sun at 17.5 nm with a spatial resolution of 20 arc-seconds, and The airglow spectrograph to measure the terrestrial FUV airgiow emissions along the horizon from 125 to 180 nm with 0.1 nm spectral resolution onboard A NASA sounding rocket experiment which launched on a "World Day", tentatively on September 23, 1992.

The ESIE consisted of a 1/4 m (EUV) spectrograph for obtaining full-disk solar irradiance. The 1/4 m spectrograph was a normal-incidence Rowland circle spectrograph with a 1 × 1024 CODACON array detector. Fig. 40 shows the solar spectrum obtained on November 10, 1988 from the ESIE. The XUV Imager consisted of a two dimensional CODACON detector with a telescope mirror and two aluminium/lexan foil filters in front of the detector. The detector array is 256 × 256 with each anode being 38 μ × 38 μ. The FUV airglow spectrograph consisted of a Wadsworth monochrometer, a telescope and a 1 × 1024 CODACON detector. The telescope was an *f*/2 CaF_2 piano-convex lens.

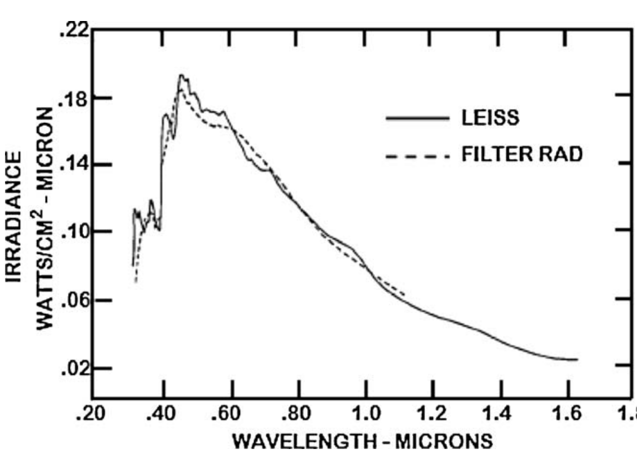


Fig. 39. Compared results of the Leiss and the filter radiometer (Webb et al. [56]).

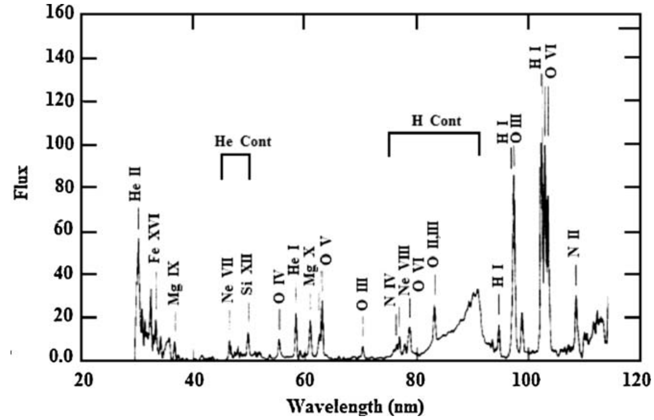


Fig. 40. The solar spectrum obtained on November 10, 1988 from the ESIE (Woods et al. [57]).

Thuillier et al. [58] used the SOLSPEC instrument to measure the solar spectral irradiance from 350 to 850 nm at 1 nm resolution during the ATLAS 1 mission. The SOLSPEC instrument was composed of three distinct spectrometers named UV, VIS, and IR. For the visible domain, the detector was a photomultiplier tube cooled 20 °C below the instrument temperature by using a Peltier effect system. The VIS spectrometer observed in eleven minutes, obtaining the solar irradiance between 340 and 850 nm in increments of 1 nm with a spectral resolution of about 1 nm. ATLAS I was launched from Kennedy Space Flight Center on 24 March 1992 by the Space Shuttle Atlantis (STS 45) and the mission ended on 2 April. Solar data were gathered during the four periods when the shuttle was oriented towards the sun. Solar data were gathered during the four periods when the shuttle was oriented towards the sun.

After applying these criteria

1. Excessive detector dark current as occurring in the South Atlantic Anomaly or when the instrument is overheated after several hours of exposure to the sun.
2. Partial absorption by the earth's atmosphere, which occurs when the line of sight (instrument to sun) has a tangent height smaller than 100 km.
3. Incomplete spectrum.
4. Unstable pointing conditions.
5. Wavelength scale instability.

From the 81 spectra recorded during the solar periods of observation, 39 spectra remained. These were obtained during day 85, 86, 89, and 91 in the year 1992, due to the better thermal conditions encountered at the beginning of each period of observations. Fig. 41a and b displays the visible spectrum together with the spectrum of Neckel and Labs (1984) measured at the Jungfraujoch, and the SSBUV data obtained on board ATLAS1 at the same time from orbit.

The study showed that the largest sources of errors were the pyrometer calibration, the weakness of the signal during calibration measurements at both ends of the spectral range and after filter changes, and finally the effect of pointing during flight. The infrared part of the SOLSPEC spectrum at 850 nm was the least accurate due to the weak signal in that region. Comparisons with other spectra showed an agreement within 2–3%, taking into account the presence of the Fraunhofer lines except below 450 nm, where discrepancies may reach five percent.

Cebula et al. [59] used the solar irradiance measurements in conjunction with the MgII proxy model to determine time-dependent instrument sensitivity changes of the Shuttle Solar Backscatter Ultraviolet (SSBUV) during eight Space Shuttle missions between

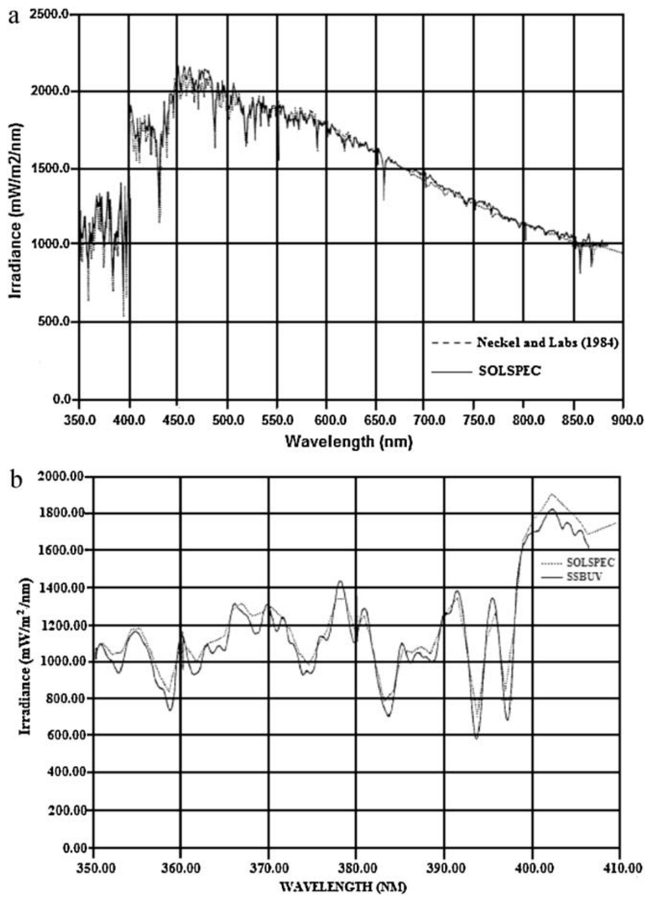


Fig. 41. (a) Absolute solar spectral irradiance from the SOLSPEC/ATLAS 1 spectrometer. (b) The spectrum of Neckel and Labs (1984) measured at the Jungfraujoch (Thuillier et al. [58]).

1989 and 1996. Reversible drifts resulted from the outgassing of the optics, while non-reversible drifts were the consequence of changes induced by solar UV radiation. These changes varied from mission to mission, but were typically less than 1% near 400 nm, increasing to 5–10% near 200 nm. During each of its missions, the SSBUV measured the solar irradiance in the spectral region from 200 nm to 405 nm at a resolution of 1.1 nm. Between three and ten separate solar-viewing periods occurred per mission, and approximately eight complete spectral scans of the sun were obtained per solar-viewing period. The dashed curve in Fig. 42 shows the ratio of

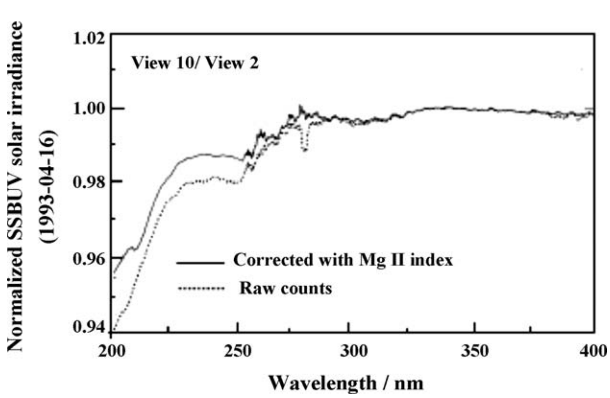


Fig. 42. The SSBUV solar irradiance counts observed on 16 April 1993 normalized to those observed on 9 April 1993. The dashed curve presents the ratio of raw counts. The solid curve presents the ratio after correcting for solar activity differences using the scaled Mg II index (Cebula et al. [59]).

the raw number of counts observed during the tenth solar-viewing period during the SSBUV-5 mission in April 1993 to that obtained during the second solar-viewing period.

Used the sun as a vicarious calibration source during each SSBUV mission, quantified, and corrected for reversible sensitivity drift due to the outgassing of the MgF2-coated optics of the instrument and irreversible sensitivity drift due to the solarization of contaminants on the diffuser had been identified.

The results showed that:

1. The application of this technique reduced the uncertainty in the SSBUV solar measurements associated with radiometric sensitivity drifts to approximately 1% at 200 nm.
2. Our results suggest that the Mg II index and scale factors can be used in the mid-UV not only as an accurate proxy for solar rotational-scale variations but also for longer, possibly solar-cycle, length variations.

Thuillier et al. [60] used the SOLar SPECtrum (SOLSPEC) and the SOlar SPectrum (SOSP) spectrometers to measure the absolute solar spectral irradiance in the range 200–2500 nm. The instrument flew in March 1992, March 1993 and November 1994 with the three ATLAS missions during 10 days. SOSP is the spare unit of SOLSPEC. It flew on the EURECA platform from 11 August 1992 to May 1993. SOLSPEC and SOSP are made of three spectrometers and contain several lamps allowing to check in flight, the instrument stability and its wavelength scale. The instruments had an identical design and were made of the same components. However, their detectors have different performance leading to SOSP responsivity smaller than the SOLSPEC responsivity. As during the ATLAS missions SSBW and SUSIM spectrometers were also observing in the UV and near visible domain.

The three SOLSPEC spectra measured in the UV region during the ATLAS missions agree for the mean within 1.5% and within 2% for the RMS above 230 nm. Below 230 nm, the solar irradiance observed during the ATLAS 2 and 3 missions was smaller than during the ATLAS 1 mission as expected due to the decreasing solar activity. The SSBW measurements agree within 2% (RMS) and 1–2% for the mean depending of the spec interval. The SUSIM spectrometer provided similar comparisons above 230 nm but there was less agreement at shorter wavelengths (>3%RMS). The visible spectra recorded during the three ATLAS missions were compared in four spectral intervals. The measurements showed consistent results in RMS difference around 1.5% and a mean difference of approximately 1%.

Using the SOLSPEC and SOSP data, they had built a solar spectrum from 200 to 2500 nm. The UV and visible parts were taken from ATLAS missions, and the infrared part from EURECA. The absolute solar spectrum at 1 AU is presented in Fig. 43 at 1 nm resolution between 200 and 870 nm, and 20 nm above.

Thuillier et al. [61] used the SOLar SPECtrum (SOLSPEC) and the SOlar SPectrum (SOSP) spectrometers to measure the absolute solar spectral irradiance in the range 200–2400 nm. SOLSPEC flew with the ATmospheric Laboratory for Applications and Science (ATLAS) while SOSP flew on the EUropean Retrieval CArrier (EURECA) missions. Both instruments were composed of three spectrometers named UV, VIS, and IR, made of a double monochromator using holographic gratings. The three spectrometers optical schematics were similar The entrance of each spectrometer was made by a quartz diffusor preceding the entrance slit The SOLSPEC instrument was turned on during the ATLAS 3 mission starting on 3 November 1993 for a ten-day duration with four periods dedicated to solar observations. A total number of 98 spectra were measured. The EURECA mission occurred from 11 August 1992 to May 1993 with the SOSP instrument on board. EURECA is an ESA platform which was placed and retrieved from orbit by the space shuttle.

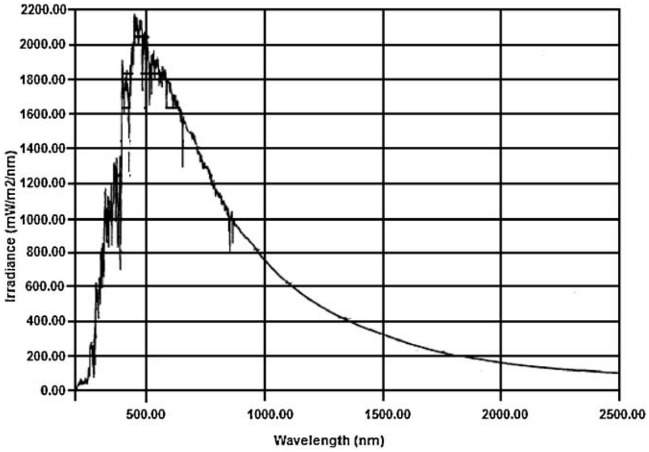


Fig. 43. The absolute solar spectrum at 1 AU is presented at 1 nm resolution between 200 and 870 nm with 20 nm resolution for longer wavelengths (Thuillier et al. [60]).

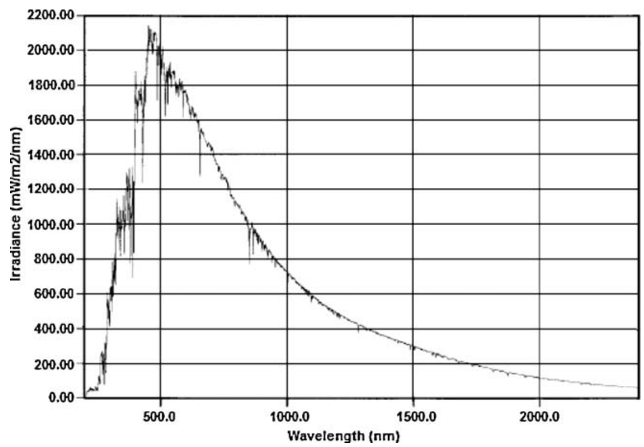


Fig. 44. Absolute solar spectral irradiance from the SOLSPEC and SOSP spectrometers from 200 to 2400 nm after normalization by 1.4% (Thuillier et al. [61]).

The data from the IR channel of the SOSP instrument were of better quality than on ATLAS for two reasons: (i) the lower responsivity avoided strong signals, and consequently non-linearity effects as observed on ATLAS, (ii) the EURECA platform remained at constant temperature (16 °C) till January 1993. Then the cooling loop was deactivated. On the other hand, the lower responsivity of the UV and visible SOSP spectrometers led us to prefer using the corresponding data from ATLAS missions. So, they used their best measurements, i.e., the UV and visible ATLAS 1 data, and the SOSP IR measurements to build a spectrum from 200 to 2400 nm as shown in Fig. 44.

5. Conclusions

The results of this review indicate:

1 Solar radiation measuring instruments can be broadband which measure the combine solar intensity at all wavelengths or spectrally selective, which measure the intensity in different wavelength bands.
2 Measurements of the solar spectral irradiance can be obtained with optical filter radiometer instruments that measure irradiance at selected narrow wavebands, and high-resolution scanning spectroradiometer, that provide full spectral information.
3 The quantity total (integrated over all wavelengths, also called “broadband”) solar irradiance is needed in the calculation of heating and cooling loads in architecture and in the design of flat-plate collectors, etc.
4 Knowledge of spectral irradiance arriving at the earth’s surface is important for the design of certain solar energy applications such as photovoltaic cells for electrical generation, and selective absorbers for thermal collectors, and for practical applications in environmental, and remote sensing applications.
5 Selected narrow wavebands instruments are characterized by simpler, less expensive and easy to maintain and calibrate compared to high-resolution scanning instruments.

References

[1] Hulstron RL. Solar resources. Massachusetts Institute of Technology; 1989.
[2] Webster JG. The measurement, instrumentation, and sensors handbook. CRC Press LLC; 1999.
[3] Igbal M. An introduction to solar radiation. New York: Academic Press Canada; 1983.
[4] Pinedo JL, Mireles F, Ríos C, Quirino LL, Dávila JI. Spectral signature of ultraviolet solar irradiance in Zacatecas. Geofísica Internacional 2006;45(4):263–9.
[5] Pecht M. Parts selection and management. John Wiley & Sons, Inc.; 2004.
[6] Calisesi Y, Bonnet RM, Gray L, Langen J, Loekwood M. Solar variability and planetary climates. Springer; 2007.
[7] Ghassemi A. Solar energy: renewable energy and the environment. Taylor & Francis Group, LLC; 2010.
[8] Lam JC, Li DH. Study of solar radiation data for Hong Kong. Energy Convers 1995;37(3):343–51.
[9] Jacovides CP, Kassomenos P, Kaltsunides NA. Estimates of effective aerosol optical depths from spectral solar radiation measurements. Theor Appl Climatol 1996;53:211–20.
[10] Singh OP, Srivastava SK, Pandey GN. Estimation of hourly global solar radiation in the plane areas of Uttar Pradesh, India. Energy Convers 1996;38(8):779–85.
[11] Souza JLD, Nicácio RM, Moura MAL. Global solar radiation measurements in Maceió, Brazil. Renew Energy 2005;30:1203–20.
[12] Islam MD, Kubo I, Ohadi M, Alili AA. Measurement of solar energy radiation in Abu Dhabi, UAE. Appl Energy 2009;86:511–5.
[13] Islam MD, Alili AA, Kubo I, Ohadi M. Measurement of solar-energy (direct beam radiation) in Abu Dhabi, UAE. Renew Energy 2010;35:515–9.
[14] Ogunjobi KO, Kim YJ. Ultraviolet (0.280–0.400 am) and broadband solar hourly radiation at Kwangju, South Korea: analysis of their correlation with aerosol optical depth and clearness index. Atmos Res 2004;71:193–214.
[15] Jacovides CP, Assimakopoulos VD, Tymvios FS, Theophilou K, Asimakopoulos DN. Solar global UV (280–380 nm) radiation and its relationship with solar global radiation measured on the island of Cyprus. Energy 2006;31:2728–38.
[16] Godish T. Air quality. CRC Press LLC; 2004.
[17] Mora SJ, Demers S, Vernet M. The effects of UV radiation in the marine environment. Cambridge University Press; 2000.
[18] Fligge M, Solanki SK, Pap JM, Fröhlich C, Wehrli Ch. Variations of solar spectral irradiance from near UV to the infrared-measurements and results. J Atmos Sol-Terr Phys 2001;63:1479–87.
[19] Lim BBP. Solar energy applications in the tropics. Holland: D. Reidel Publishing Company; 1983.
[20] Wehrli Ch, Frohlich C. Solar spectral irradiance measurements at 368 nm, 500 nm and 778 nm. Metrologia 1991;28:285–9.
[21] Wehrli Ch, Fröhlich C, Romero J. Results of solar spectral irradiance measurements by sova2 on eureka. Adv Space Res 1995;16(8):25–8.
[22] Rabbette M, Pilewskie P. Multivariate analysis of solar spectral irradiance measurements. J Geophys Res 2001;106:9685–96.
[23] Laue EG. The measurement of solar spectral irradiance at different terrestrial elevations. Sol Energy 1969;13:43–57.
[24] Michalsky JJ, Kleckner EW. Estimation of continuous solar spectral distributions from discrete filter measurements. Sol Energy 1984;33(1):57–64.
[25] Michalsky JJ. Estimation of continuous solar spectral distributions from discrete filter measurements: II. A demonstration of practicability. Sol Energy 1985;34(6):439–45.
[26] King DL, Kratochvil JA, Boyson WE. Measuring solar spectral and angle-of-incidence effects on photovoltaic modules and solar irradiance sensors. In: IEEE Photovoltaic Specialists Conference. 1997.
[27] Stair R, Johnston G. Preliminary spectroradiometric measurements of the solar constant. J Res Natl Bur Stand 1956;57(4):205–11.
[28] Mecherikunnel A, Duncan CH. Total and spectral solar irradiance measured at ground surface. Appl Opt 1982;21(3):554–6.
[29] Thuillier G, Goutail JP, Simon PC, Pastiels R, Labs D, Neckel H. Measurement of the solar spectral irradiance from 200 to 3000 nanometers. Science 1984;225:182–4.
[30] Cannon TW. Spectral solar irradiance instrumentation and measurement techniques. Sol Cells 1986;18:233–41.
[31] Riordan C. Spectral solar radiation data and measurements. Sol Cells 1988;24:313–20.

[32] Manjul SS, Verma SD. Ground based multitemporal measurements of global solar spectral irradiance and estimation of atmospheric transmittances. Opt Sensors 1992;1814:175–82.

[33] Martinez-Lozano JA, Utrillas MP, Tena F. Spectral solar irradiance in the range 300–1100 nm measured at Valencia, Spain. Renew Energy 1995;6(8):997–1003.

[34] Adeyefa ZD, Holmgren B, Adedokun JA. Spectral solar irradiance under Harmattan conditions. Renew Energy 1995;6(8):989–96.

[35] Adeyefa ZD, Holmgren B. Spectral solar irradiance before and during a Harmattan dust spell. Sol Energy 1996;57(3):195–203.

[36] Adeyefa ZD, Holmgren B, Adedokun JA. Spectral solar radiation measurements and turbidity: comparative studies within a tropical and a sub-arctic environment. Sol Energy 1997;60(1):17–24.

[37] Bernhard G, Mayer B, Seckmeyer G, Moise A. Measurements of spectral solar UV irradiance in tropical-Australia. J Geophys Res 1997;102:8719–30.

[38] Bruce CK, Qu Z, Goetz AFH. Direct solar spectral irradiance and transmittance measurements from 350 to 2500 nm. Appl Opt 2001;40(21): 3483–4394.

[39] Pérez-López JJ, Fabero F, Chenlo F. Experimental solar spectral irradiance until 2500 nm: results and influence on the PV conversion of different materials. Prog Photovolt: Res Appl 2006;15:303–15.

[40] Krezhova DD, Yanev TKTK, Krumov AH. Solar radiation dynamics during the total solar eclipse on 11 August 1999 in the Territory of Bulgaria. Sun Geosphere 2007;2(1):56–60.

[41] Krezhova DD, Krumov AH, Yanev TK. Spectral investigations of the solar radiation during the total solar eclipse on March 29, 2006. J Atmos Sol-Terr Phys 2008;70:365–437.

[42] Polo J, Zarzalejo LF, Salvador P, Ramírez L. Angstrom turbidity and ozone column estimations from spectral solar irradiance in a semi-desertic environment in Spain. Sol Energy 2009;83:257–63.

[43] Coulson KL. Solar and terrestrial radiation methods and measurements. Academic Press, Inc.; 1975.

[44] Kimlin MG, Taylor TE. Comparison of the plant-damaging spectral solar ultraviolet radiation between three locations in Eastern USA in the year 2000. Agric Forest Meteorol 2003;120:83–100.

[45] Helbling EW, Zagarese HE. UV effect in aquatic organisms and ecosystems. The Royal Society of Chemistry; 2003.

[46] Driscoll CMH. Solar UVR measurements. Radiat Prot Dosim 1996;64(3):179–88.

[47] Wong Jc, Parisi AV. Measurement of UVA exposure to solar radiation. Photochem Photobiol 1996;63(6):807–10.

[48] Roy CR, Gies HP, Lugg DJ, Toomey S, Tomlinson DW. The measurement of solar ultraviolet radiation. Fundam Mol Mech Mutagen 1998;422:7–14.

[49] Mikhalev AV, Chernigovskaya MA, Beletsky AB, Kazimirovsky ES, Pirog OM. Variation of the ground-measured solar ultraviolet radiation during the solar eclipse on March 9, 1997. Adv Space Res 1999;24(5):657–60.

[50] Parisi AV, Kimlin MG. Horizontal and sun-normal spectral biologically effective ultraviolet irradiances. J Photochem Photobiol 1999;53:70–4.

[51] Feister U, Gericke K. Cloud flagging of UV spectral irradiance measurements. Atmos Res 1998;49:115–38.

[52] Gröbner J, Blumthaler M, Kazadzis S, Bais A, Webb A, Schreder J, et al. Quality assurance of spectral solar UV measurements: results from 25UV monitoring sites in Europe, 2002 to 2004. Metrologia 2006;43:66–71.

[53] Ren PB, Gjessing Y, Sigernes F. Measurements of solar ultra violet radiation on the Tibetan Plateau and comparisons with discrete ordinate method simulation. J Atmos Sol-Terr Phys 1999;61:425–46.

[54] Kazadzis S, Bais1 A, Blumthaler M, Webb A, Kouremeti N, Kift R, et al. Effects of total solar eclipse of 29 March 2006 on surface radiation. Atmos Chem Phys 2007;7:5775–83.

[55] William C, Dickinson C. Solar energy technology handbook. Marcel Dekker, Inc.; 1980.

[56] Webb JJ, Duncan CH, McIntosh R, Lester D. Solar spectral irradiance measured from 11.58 km with a Leiss monochromator and a photoelectric filter radiometer. Appl Opt 1970;9(2):345–9.

[57] Woods TN, Bailey SM, Solomon SC, Rottman GJ. Far ultraviolet and extreme ultraviolet rocket instrumentation for measuring the solar spectral irradiance and terrestrial airglow. SPIE 1992;1745:140–8.

[58] Thuillier G, Herŝe M, Simon PC, Labs D, Mandel H, Gillotay D, et al. The visible solar spectral irradiance from 350 to 850 nm as measured by the solspec spectrometer during the atlas I mission. Sol Phys 1998;177:41–61.

[59] Cebula RP, Huang LK, Hilsenrath E. SSBUV sensitivity drift determined using solar spectral irradiance measurements. Metrologia 1998;35: 677–83.

[60] Thuillier G, Hersé M, Simon PC, Labs D, Mandel H, Gillotay D, et al. The absolute solar spectral irradiance from 200 to 2500 nm as measured by the SOLSPEC spectrometer with the ATLAS and EURECA missions. Phys Chem Earth (C) 2000;25(5–6):375–7.

[61] Thuillier G, Hersé M, Labs D, Foujols T, Peetermans W, Gillotay D, et al. The solar spectral irradiance from 200 to 2400 nm as measured by the solspec spectrometer from the atlas and eureca missions. Sol Phys 2003;214:1–22.